COLLINS, DAVIS EARL, M.S. Investigating the Inhibition of Cytochrome P450 Isoform 1A1 by Açai Berry (Euterpe oleracea) Extracts Using a Bioassay Guided Fractionation Approach. (2016)
Directed by Dr. Gregory M. Raner. 90 pp.

Xenobiotic metabolism is an important process within the human body, as it alters large, foreign, hydrophobic molecules and prepares them for excretion. This process is largely carried out in the liver and is accomplished by a superfamily of heme-containing enzymes, termed the Cytochrome P450's. Each individual P450 has a certain specificity for the substrates it may metabolize, but these enzymes are non-selective in nature and may catalyze the metabolism of a wide variety of substrates. Due to this characteristic of P450 – mediated metabolism, pharmaceuticals when taken concomitantly may possibly interfere with one another's metabolism, which can lead to adverse drug reactions. This can also be true for natural product constituents that have been consumed as a part of one's dietary intake. Consumption of the açai berry (*Euterpe oleracea*) has grown quite rapidly in recent years as it contains a high concentration of antioxidant molecules, and has also been marketed as a weight loss supplement. Although it appears to benefit one's health and longevity, the açai berry has not been characterized in terms of its effect on P450 – mediated metabolism. Utilizing an activity guided fractionation scheme, açai berry extracts were assayed in CYP1A1 and CYP1A2 enzyme reactions to determine constituents responsible for enzyme inhibition.

INVESTIGATING THE INHIBITION OF CYTOCHROME P450 ISOFORM 1A1 BY AÇAI BERRY (EUTERPE OLERACEA) EXTRACTS USING A BIOASSAY GUIDED FRACTIONATION APPROACH

by

Davis Earl Collins

A Thesis Submitted to
the Faculty of The Graduate School at
The University of North Carolina at Greensboro
in Partial Fulfillment
of the Requirements for the Degree
Master of Science

Greensboro
2016

Approved by

_____
Committee Chair

APPROVAL PAGE

This thesis written by Davis Earl Collins has been approved by the following committee of the Faculty of The Graduate School at The University of North Carolina at Greensboro.

Committee Chair _____

Committee Members _____

_____

_____
Date of Acceptance by Committee

_____
Date of Final Oral Examination

TABLE OF CONTENTS

Page

LIST OF TABLES

Page

LIST OF FIGURES

Page

LIST OF EQUATIONS

Page

LIST OF SCHEMES

CHAPTER I

INTRODUCTION

1.1.0 Xenobiotic Metabolism

Xenobiotic metabolism is a vital process within a living organism, as it methodically alters any consumed, foreign molecules and prepares them for excretion. These molecules can be either large or small, polar or non-polar, and toxic or non-toxic. This process often involves the oxidation of non-polar species, which renders them slightly more polar and soluble in water. These compounds may be ingested via a variety of vectors such as pharmaceuticals, constituents consumed from one's daily dietary intake, or exposure to environmental pollutants[1]. It is of utmost physiological importance to eliminate these exogenous compounds from the human body, as high systemic concentrations may lead to deleterious or even life – threatening side effects[2]. Degradation of these compounds is accomplished by two different phases.

Phase I metabolism is largely carried out by a superfamily of heme – containing enzymes named the Cytochromes P450. The heme, which is located in the active site of these enzymes, is able to bind and activate molecular oxygen to react with a substrate molecule. These enzymes are characterized as monooxygenases, and a general monooxygenase reaction can be seen in Equation 1. Although there is some specificity as to what substrates a certain

CYP enzyme will metabolize, these enzymes are non – selective in nature and can interact with a plethora of different molecules[3]. The duration of a foreign molecule's clearance from the body is majorly affected by the rate at which one or more CYP enzymes catalyze its degradation[4]. Metabolites generated from phase I metabolism are generally polar and are excreted via the renal system, as polar molecules typically do not bind with plasma proteins in the blood and are filtered out within the kidney[5].

Phase II metabolism involves the conjugation of xenobiotics or their metabolites, oxidative byproducts, or toxic species to biomolecules such as glucose, sulfate, or glutathione[4]. This phase of the pathway is responsible for neutralizing chemical species that the body does not recognize as an endogenous compound. Metabolites formed as a result of phase II metabolism are conjugated, which results in an increased molecular weight, as well as polarity. A common route of elimination for these compounds is via the intestines. These compounds are excreted by the liver into bile found within the gallbladder; once contained in the bile, they are secreted into the intestinal tract and eliminated in the feces. However, some enzymes located in the intestinal flora are capable of hydrolyzing certain glucuronide or sulfate conjugates, which in result releases the less-polar compound, and renders it available for reabsorption. This process is known as enterohepatic circulation, and prolongs the lifetime of the xenobiotic within the body[5].

$$RH + O_2 + NADPH \rightarrow ROH + H_2O + NADP^+$$

Equation 1. General Reaction of Cytochrome P450.

1.2.0 Cytochrome P450's

A large portion of these drug – metabolizing enzymes belong to the Cytochrome P450 superfamily, which were first identified within the endoplasmic reticulum of hepatocytes by J. Axelrod and B. Brodie *et al.*, in 1955[6,7]. They form a class of ubiquitous, membrane – bound enzymes, which are found in either cellular endoplasmic reticulum or mitochondrial membranes, and are present throughout many forms of life[8]. The term P450 corresponds to the unique absorption spectrum observed when the enzyme is complexed with carbon monoxide; first demonstrated in 1958 by Garfinkle using pig liver, and Klingenberg using rat liver, the CO complexed enzyme displays a maximum absorbance when exposed to a wavelength of 450 nm[9,10].

Within this superfamily of enzymes, there are many individual enzymes, which are termed isozymes. Although isozymes may have many characteristics in common, minute differences in their genomic or amino acid sequence, substrates that they may metabolize, and their three – dimensional structure give rise to the unique properties of an individual enzyme[11]. Isozymes are named using a three character identification system followed after the CYP abbreviation, which is classified based on genome sequence homology. For example, CYP1A1, would denote that this isozyme belongs to the '1' family, the '1A'

subfamily, and the final '1' refers to the specified enzyme species within that subfamily.

1.2.1 Cytochrome P450 Active Site And Catalytic Cycle

One highly conserved feature of CYP450 enzymes is their heme – containing active site, which is essential in the oxidative catalysis of CYP450 substrates[12]. This 'heme' is a porphyrin molecule containing an iron atom, which is located within the center of the structure. Below in Figure 1 shows several of the oxidative species involved in CYP450 enzymatic reactions; the ferric iron center is able to activate molecular oxygen (O_2) via a method shown below in Figure 2. Displacement of an active site water molecule by a substrate molecule, RH, is the initial step in this process (***1***). The ferrous iron center gains an electron, which reduces it to the ferrous state (***2***) capable of binding to molecular oxygen (***3***). A newly formed iron-oxo radical is further reduced by addition of another electron (***4***). An oxygen atom is then protonated generating a water molecule, which leaves the active site and creates a double bond between the remaining oxygen atom and the iron center (***5***). Through this activation cycle the enzyme is able to generate an extremely reactive oxygen species that is capable of oxidizing virtually any organic compound[13] (***6***). Direct binding of a peroxide molecule to the unbound ferric center is another possible means of activation (**2***). With this being said, CYP450 enzymes are non – selective in nature and can catalyze a plethora of reactions, pending the availability of a given substrate within an enzyme's active site[14].

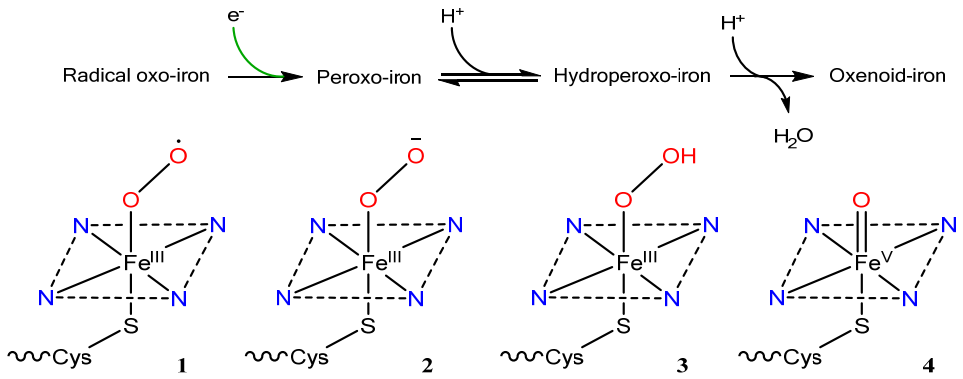

Figure 1. Oxidative Species of the CYP450's[15]. The heme iron is able to utilize oxygen as a radical (1), nucleophile (2, 3), and electrophile (4).

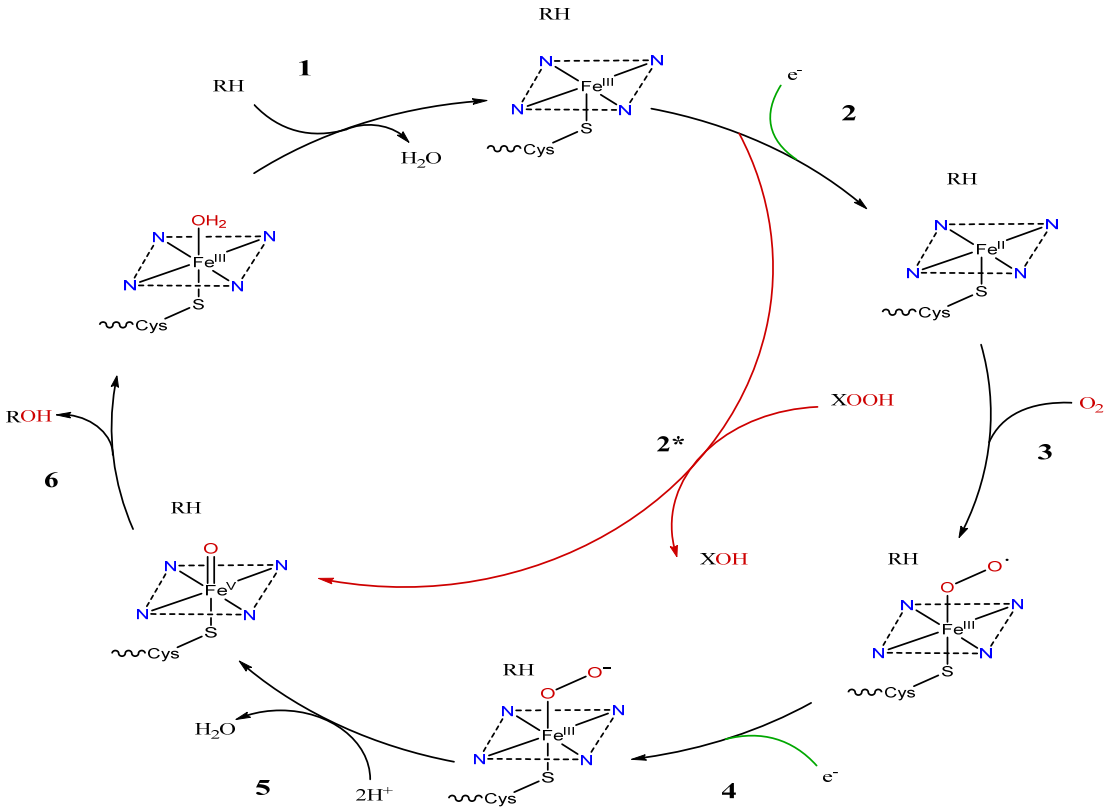

Figure 2. Catalytic Cycle of a CYP450 Monooxygenase Reaction. This cycle is thought to be conserved in nearly all P450 species.

Structural differences that arise from the various genomic sequences of the CYP450 superfamily play the ultimate role of allowing different substrates access to the various active sites. Size, shape, and arrangement of functional groups of the active site are primarily what give rise to an enzyme's affinity for a substrate molecule[16].

1.2.2 Hydroxylation of Hydrocarbon Molecules

One of the most basic, as well as most common monooxygenase reactions catalyzed by the CYP450's, is the hydroxylation of a sp^3 carbon. This reaction, which is shown below in Figure 3, is a two – step radical mechanism. First a hydrogen atom is abstracted by the oxo-ferryl group in the Fe(V) oxidation state, which leaves a radical carbon of where the hydrogen was abstracted[17]. A step termed "oxygen rebound" happens immediately following the hydrogen abstraction, as the hydroxyl group on the heme transfers to the formed radical carbon. A hydroxylated product is formed from this reaction, and returns the enzyme back to its resting ferric state[17].

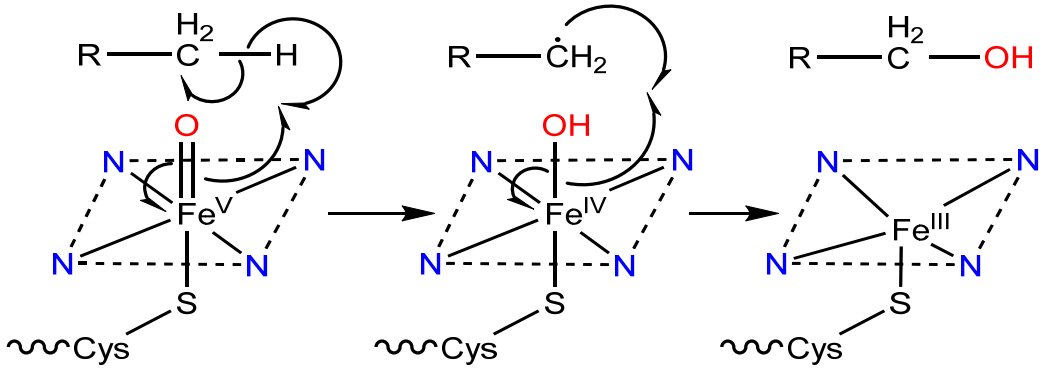

Figure 3. Hydrocarbon Hydroxylation Reaction. Primary reaction of CYP450 enzymes, using a two-step radical mechanism.

1.2.3 Heteroatom Dealkylation

Substrates involving a target carbon located adjacent to a nitrogen, oxygen, or sulfur typically undergo CYP450 mediated hydroxylation, and results in the oxidation and dealkylation of the substrate. This reaction is important as the substrate probe used in both 1A1 and 1A2 enzyme reactions, is an ether molecule. Shown in Figure 4 is the accepted mechanism of this reaction. Due to the proximity of the newly added hydroxyl group to the adjacent heteroatom, the product molecule undergoes an intramolecular reaction that results in the formation of the final product, as well as a secondary metabolite, which is usually an aldehyde molecule[18].

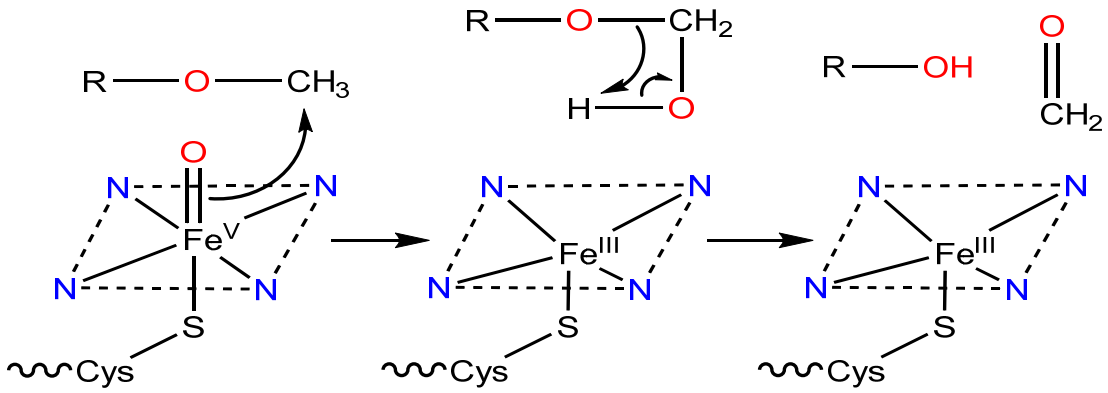

Figure 4. Dealkylation of Heteroatom Molecules. Hydrogen abstraction followed by oxygen rebound, resulting in the product of interest (ROH) and a formaldehyde molecule.

1.3.0 Kinetics of Cytochrome P450 – Mediated Drug Metabolism

Using the Michaelis – Menten model of enzyme kinetics it is possible to relate the velocity of an enzymatic reaction to the concentration of substrate present. Upon substrate (S) binding to an enzyme's active site (E), an enzyme – substrate complex (ES) is created. This complex undergoes catalysis to yield a product, as well as a regenerated enzyme. The rates at which these steps take place while the reaction is at "steady – state," allows the prediction of important physical parameters such as the K_m and V_{max}. An equation that is representative of this concept is shown as follows in Equation 2:

$$\mathbf{v = (V_{Max}\,[S]) / (K_m + [S])}$$

Equation 2. Michealis – Menten Model of Enzyme Kinetics Equation.

This equation is plotted along an XY axis that is shown in Figure 5 and follows a rectangular hyperbolic relationship, which appears roughly linear at low substrate concentrations, but asymptotically approaches a maximum velocity (V_{max}). This V_{max} term reflects conditions at which an enzyme is at its maximum rate of product formation, due to the complete saturation of the enzymes with substrate. The substrate concentration at which the velocity of the enzymatic reaction is 50% of its maximum is termed the K_m and is another important constant in Michaelis – Menten kinetics. At this substrate concentration, 50% of enzymes within a reaction have a substrate molecule bound to its active site. When developing and optimizing an enzymatic bioassay, it is imperative to use a substrate concentration in close proximity to the K_m value, as changes in the rate of product formation are most apparent under these conditions.

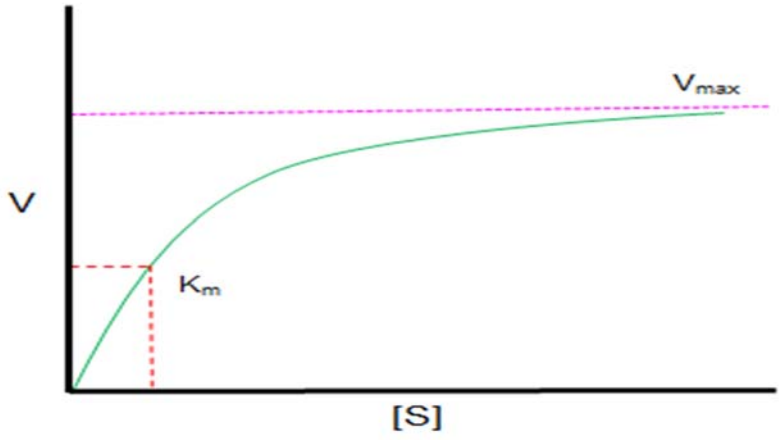

Figure 5. Michealis – Menten Plot. Illustration of the rectangular hyperbolic relationship between reaction velocity (V) and substrate concentration [S], also shows two important parameters K_m and V_{max}.

1.3.1 CYP450 Inhibition

As mentioned previously, CYP450 molecules serve to remove and detoxify foreign compounds ingested within the human body[2]. As with any enzyme, when in the presence of competing substrate molecules or related compounds, the activity towards a single substrate is reduced. The purpose of this project is to investigate inhibition of CYP450 isoforms by constituents found in the açai berry, which has gained much attention as of late for its positive health effects[19-23]. An enzyme inhibitor is any molecule that decreases an enzyme's efficacy, and alters the metabolism of another molecule's metabolism. Inhibition can be either a reversible or irreversible process. Reversible inhibition involves an enzyme's affinity for another substrate molecule, and only lasts as long as the inhibitor is present[24]. Irreversible inhibition occurs when an inhibiting molecule binds covalently to the active site or a key amino acid residue. Reactive metabolites generated from CYP450 catalysis can also affect the enzyme in this manner, in a process known as "suicide inhibition," and will permanently remove the affected enzyme from the catalytic enzyme pool. An equation used to calculate K_I for competitive inhibition is shown below in equation 3. In this equation the term denoted α is representative of the ratio between the K_m value observed in a controlled experiment with no inhibitor and the $K_{m\ app}$ observed in experimental reactions. This value, which can be determined experimentally, is equal to the concentration of inhibitor ([I]) divided by K_i, plus 1. Rearrangement

of the equation to solve for K_i yields a value reflective of the inhibitors binding affinity with the enzyme.

$$\alpha = (K_{m\ app} / K_m) = 1 + ([I] / K_i)$$

Equation 3. K_i Determination for a Competitive Inhibitor.

1.4.0 Drug Interactions and Adverse Drug Reactions In CYP450 Isoforms

It is of considerable interest to study cytochrome P450 interactions due to the wealth of both prescription and over the counter medications produced by the flourishing pharmaceutical industry. As healthcare is becoming more attainable to the average citizen, there has been an enormous increase in the number of prescriptions written every day, and as a result it is not by chance that there has been an increase in the number of reported adverse drug reactions[25]. Cytochrome P450 enzymes are non – selective in nature, which means that a certain isoform may metabolize a wide variety of substrates of related size, structures, or chemical properties[26]. In the following sections more detail is given about known CYP1A1 and CYP1A2 substrates, as well as some specific examples of adverse side effects of CYP1A1 and CYP1A2 mediated drug metabolism.

1.4.1 CYP1A1

Cytochrome P450 isoform 1A1 is, for the most part, an extrahepatic enzyme, although, it can be expressed within the liver. CYP1A1 has relevance not so much as a drug metabolizer, but rather as a metabolizer of endogenous

substrates and is an important detoxifier of environmental pollutants. Environmental pollutants are typically highly nonpolar molecules, and can be consumed via inhalation from the air or ingested from foods eaten as part of a normal diet. CYP1A1 is largely studied in works interested in cancer prevention. This is because many of CYP1A1's natural substrates are highly nonpolar and unreactive, but once subjected to CYP1A1 mediated metabolism, become much more reactive resulting from the addition of the heteroatom function group. These newly formed reactive products can attack cellular structures, such as DNA, which form DNA adducts that can affect the integrity of the DNA sequence[26]. This process has been termed "carcinogenesis," as it is the process by which a cancer line can arise. With this being said, it is of interest to potentially inhibit reactions of CYP1A1 in an attempt to impede the generation of these highly reactive products. Depicted below in Table 1, is a list of endogenous and exogenous substrates of CYP1A1, as well as some known inhibitors.

Table 1. List of Known Substrates and Inhibitors of CYP1A1[26, 27, 28]

ENDOGENOUS CYP1A1 SUBSTRATES			
arachidonic acid	*eicosapentoic acid*	*17β-estradiol*	*melatonin*
EXOGENOUS CYP1A1 SUBSTRATES			
combustion/tobacco products	*heterocyclic aromatic amines*	*industrial aryl amines*	*polycylcic aromatic hydrocarbons*
granisetron			
KNOWN CYP1A1 INHIBITORS			
alizarin	*fluvoxamine*	*miconazole*	*pyrene*
bergamotin	*lidocaine*	*α-napthoflavone*	*resveratrol*
cannabinoids	*luotonin A*	*β-napthoflavone*	*zileuton*

1.4.2 CYP1A2

Cytochrome P450 isoform 1A2 is largely a hepatic enzyme, and has been said to account for approximately 13% of CYP450 enzymes found in the liver[29]. Although this percentage can vary highly among individuals, CYP1A2 is an important metabolizer of several known prescription drugs, as well as environmental toxins and procarcinogens[30]. Recent studies have shown that CYP1A2 is more heavily involved in pharmaceutical drug metabolism than originally believed to be. Many of these drugs, such as Zolmitriptan, a selective serotonin receptor agonist used to alleviate migraine headaches,[31] and Tacrine an anticholinesterase used in Alzheimer's treatments[32], are medications prescribed for CNS disorders. In most cases a drug molecule will be metabolized by several different CYP450 isoforms, but this is not always the case. It is also of importance to realize that when CYP1A2 is in the presence of several of its substrates, these substrates of CYP1A2 can act as competitive

inhibitors of one another via competition to enter the enzyme's active site[33].

Below in Table 2, is a list of known CYP1A2 substrates and inhibitors.

Table 2. List of Known Substrates and Inhibitors of CYP1A2[34]. Strong inhibitors are denoted in red, while mild inhibitors are denoted in yellow.

CYP1A2 SUBSTRATES				
amitriptyline	*estradiol*	*naproxen*	*propranolol*	*tizanidine*
caffeine	*fluvoxamine*	*olanzapine*	*riluzole*	*verapamil*
clomipramine	*haloperidol*	*ondansetron*	*ropivacaine*	*(R)warfarin*
clozapine	*imipramine N-DeMe*	*phenacetin*	*tacrine*	*zileuton*
cyclobenzaprine	*mexilletine*	*acetaminophen → NAPQI*	*theophylline*	*zolmitriptan*
CYP1A2 INHIBITORS				
amiodarone	*efavirenz*	*fluvoxamine*	*interferon*	*mibefradil*
cimetidine	*fluoroquinolones*	*furafylline*	*methoxsalen*	*ticlopidine*
ciprofloxacin				

1.4.3 Oxidative Stress

Although xenobiotic metabolism has an overall beneficial effect, due to the means by which this process occurs (using molecular oxygen as an oxidizing agent) metabolism of certain drugs, such as acetaminophen, can generate reactive metabolites as by-products of the reaction[35]. An accumulation of these oxidative species can lead to an imbalanced ratio of antioxidants to oxidants[36]. This imbalance can cause oxidative damage to surrounding cells, through reaction of activated metabolites with complex cellular molecules such as, nucleotides, proteins, and lipids[37, 38]. In other words, Cytochrome P450 enzymes in humans can detoxify and eliminate foreign chemicals, but they can also convert inert chemical species into toxic metabolic products.

1.4.4 CYP1A2 Metabolism of Acetaminophen

In the case of acetaminophen, overdose poses a serious threat of hepatotoxicity, because the secondary (toxic) route for metabolism becomes significant at elevated drug levels. This compound is a non-steroidal anti-inflammatory drug (NSAID) that is taken to alleviate fevers, headaches, and other minor pains caused by inflammation. Although it is considered safe at therapeutic dosages, an overdose of this drug is extremely toxic to liver cells and is a major cause of acute liver failure in the United States[39]. A diagram depicting the usual route of elimination is shown below in Figure 6. It has been shown that at therapeutic dosages, acetaminophen is mainly eliminated in the liver by glucuronidation and sulfation reactions[40]. Acetaminophen is also metabolized by CYP isoforms 2E1, 1A2, 3A4, and 2D6 [41]. P4502E1 mediated metabolism of acetaminophen is a direct two electron oxidation, that results in the formation of N-acetyl-p-benzoquinone imine (NAPQI), which is an extremely reactive metabolite[35]. NAPQI is a strong electrophile and is rapidly reduced by GSH into an acetaminophen-GSH conjugate. Upon consumption of a toxic dose of acetaminophen, its NAPQI metabolite readily depletes hepatic GSH concentrations. This depletion results in NAPQI covalently binding to nucleophilic groups of important cellular proteins[42]. Covalent alteration of these proteins can cause reduced or impaired activity of necessary cellular functions. Depletion of hepatic GSH may also result in an accumulation of peroxides in cells, as glutathione peroxidase, a major peroxide detoxification pathway, cannot

proceed without its necessary cofactor GSH[39]. Oxidative stress in the cell resulting from acetaminophen overdose has also been shown to have an effect on mitochondrial permeability transition[43], which can also contribute to acute liver failure. Acetaminophen overdose is but one example of how oxidative stress produced as a result of drug metabolism can cause localized tissue damage. Although this case is one of the more severe and thus most studied incidents of drug induced hepatotoxicity, metabolism of other drug compounds may cause milder conditions of oxidative stress. Over time, exposure to elevated levels of oxidants and ROS can cause chronic liver inflammation.

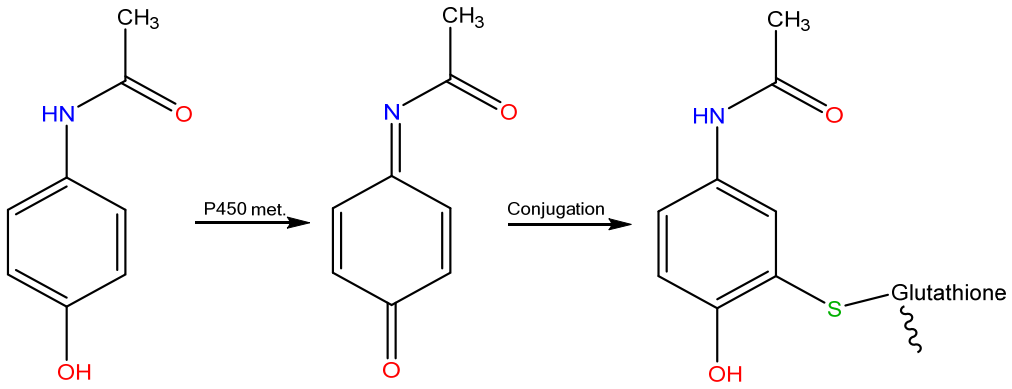

Figure 6. CYP450 Catalysis of Acetaminophen Followed by Phase II Conjugation. Usual degradation under physiological conditions and low doses of acetaminophen.

1.4.5 CYP1A1 Bioactivation of Procarcinogens

Acquisition of many forms of cancer have been associated with exposure to environmental pollutants, via inhalation and even consumed within one's diet. Much is known of the mechanisms underlying cancer initiation, as well as many chemicals that can be responsible (carcinogens). A large portion of these carcinogens are aldehydes or other volatile organic compounds[44]. Two other classes of carcinogens are the polycyclic aromatic hydrocarbons (PAH), such as benzo[a]pyrene, and the tobacco specific nitrosamines (TSN), such as 4-(methylnitrosamino)-1-(3-pyridyl)-1-butanone; which are debatably the two of the most important compounds in lung carcinogenesis[45].

As with any foreign, hydrophobic, compound that enters the body via the gastrointestinal tract, it is subject to first pass metabolism by the CYP enzymes[1]. Despite that many PAHs are not considered actual carcinogens, CYP oxidation of these compounds often results in the formation of reactive products. Under usual circumstances these metabolites are eliminated from the body by phase II processes, largely by forming glutathione complexes[3]. However, when concentrations of glutathione are depleted electrophilic intermediates covalently bind to DNA forming adducts which may cause mutations within the genome. Over time damaged DNA is unable to be repaired and the sequence becomes increasingly replicated, leading to tumorgenesis[26]. Since it is the CYP metabolism of PAHs that is responsible for the generation of a reactive product, inhibition of certain CYP isozymes that are known to catalyze these reactions

appears to be a logical approach to ameliorate DNA damage that may ultimately lead to cancer. Isoforms known to activate carcinogens include mainly CYP1A1, but CYP1A2 has also been shown to be involved in this process.

1.5.0 Natural Products and CYP450's

It is well known that natural products can have beneficial health effects, and there is considerable interest in antioxidant properties of many of these products. The origins of the medicinal use of these natural products can often be traced back thousands of years, as herbal products were mainly used in traditional medicine. Through the process of trial and error, indigenous civilizations experimented with the local plants to determine the medicinal effect that they might have. With the rise of modern medicine and biochemical research during the past two or three decades, techniques have been developed to distinguish medicinally active compounds and unravel their complex molecular mechanisms. Much effort has been focused on natural products due in part to successful accounts of folklore medicine, but largely because the synthesis of medicinally active constituents is "programmed" within a species' genome, and was possibly critical to its survival, as it has been evolutionarily conserved.

During recent years herbal products have gained increasing popularity, as they can prove beneficial to one's health in numerous ways. In 2005, it was reported by Tindle et al. that 12.1 – 18.6% of adults in the United States used herbal remedies[46], and this number has only increased in the past ten years as these products have been made much more available. Because herbal drugs

are obtained from a natural, plant source, these remedies are often perceived as "safe"; but herbal products are a complex mixture of organic constituents, whose elimination from the human body is facilitated by the same xenobiotic metabolism process as synthetic drugs[47]. Despite providing a natural, holistic approach to maintaining one's health and longevity, many of these natural products have not been characterized in terms of their effect on CYP450 enzymes and other biochemical processes[24]. It is of much interest to the healthcare and pharmaceutical industries to identify any significant natural product – drug interactions, as it is a means to proactively prevent possible adverse drug reactions.

1.5.1 Herbal Drug – Pharmaceutical Drug Interactions

It has also been shown that certain fruits may interfere with normal drug metabolism. Concomitant intake of herbal products and prescription medication was estimated at 16% during the year 2002[48]. A classic example is the interaction of grapefruit with the CYP3A4 isoform. CYP3A4 is responsible for the metabolism of a large percentage of all pharmaceutical drugs[24]. It has been shown that furanocoumarins found in grapefruit are metabolized by this enzyme to generate a reactive metabolite, which then covalently binds to CYP3A4 causing irreversible inhibition[49]. These furanocoumarin constituents are specifically bergamottin and 6',7'-dihydroxybergamottin[50], and their corresponding structures can be found below in Figure 7. This interaction is significant as drugs taken simultaneously with the consumption of grapefruit may

not be fully metabolized and may cause undesirable side effects, or in severe cases even drug overdose. A well – studied example is grapefruit's interaction on the metabolism of statin drugs, which are widely prescribed cholesterol modulators[51]. Alteration of statin drug metabolism greatly affects these medicines' pharmacokinetic and pharmacodynamics properties, which can cause an adverse drug reaction. Atorvastatin (Lipitor), which is the highest grossing drug of all time[52], belongs to this class of drugs; so it is imperative that these interactions are made known to the pharmaceutical and healthcare industries.

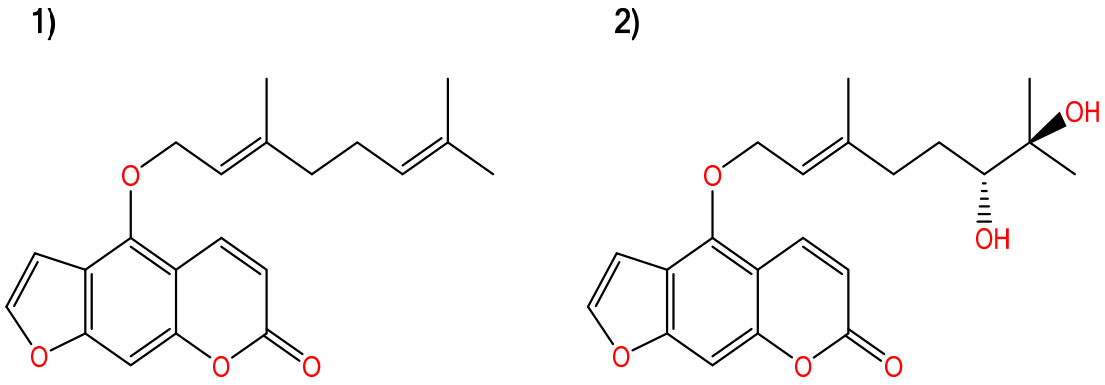

Figure 7. Structures of Bergamottin and 6',7'-Dihydroxybergamottin. BG (1) and DHB (2) are the constituents in grapefruit responsible for CYP3A4 inhibition.

1.5.2 Chemopreventative Qualities

A major question within the natural product community throughout the 1990's was the biochemical correlation between the relatively high resveratrol concentrations found in red wine and the documented cardioprotective effects from its consumption; a conundrum termed the "French Paradox"[53]. Initial research focused on metabolic processes of the cardiovascular system, but it

was shown in animal models of carcinogenesis that resveratrol exerts potent chemopreventative effects[54]. Much research has been geared towards understanding the biochemical mechanisms that link together the many ways by which resveratrol exerts its chemopreventative, cardiovascular, and neuroprotective effects[55].

As mentioned previously, CYP1A1 metabolism of procarcinogenic compounds results in the generation of carcinogens. Upon ingestion of a PAH, it binds to the aryl hydrocarbon receptor (AhR), which induces the transcription of CYP1A1 proteins in an effort to detoxify the body of these foreign compounds. However, this metabolism creates a highly reactive product which is capable of covalently binding to DNA, forming DNA adducts that can affect the integrity of the DNA sequence[26]. Much work has been done evaluating the effects of flavonoids and other dietary polyphenols in cell culture models of both cancer initiation and promotion[55, 56, 57]. *In vitro* studies investigating flavonoids and other polyphenols effect on the cancer initiation stage have shown this class of natural products greatly affects many steps necessary for the bioactivation of carcinogens and the covalent binding of the carcinogen to DNA[58]. This has been shown to happen via a variety of different mechanisms; some acting as agonists of AhR inducing CYP1A1 transcription, while others may act as antagonists of AhR and inhibit the transcription of the bioactivating oxidative enzymes[59, 60, 61].

Although the results of many of these *in vitro* studies appear promising, uncovering a cellular mechanism by which these polyphenols exert their effect

has proven to be more complex than originally expected. Also, *in vivo* studies evaluating the effect of flavonoids and polyphenols have been rather disappointing. This is most likely due to the poor bioavailability of these compounds, as they undergo degradation within the gastrointestinal tract and will not reach internal organs at a sufficient concentration[62, 63]. However, a subclass of these polyphenolic compounds, the methoxylated flavones have proven to have a considerably greater potential to reach their target tissues compared to their unmethylated counterparts. It has been shown that both 3,4-dimethoxyflavone and 5,7-dimethoxyflavone can act as an antagonist of AhR, as well inhibit the CYP450 bioactivation of benzo[α]pyrene at fairly low concentrations (1 – 2 μM)[64].

1.5.3 Açai Berry

There has been a recent increase in the consumption of Açai berry, as it is widely available in dietary supplements and in some antioxidant drinks. It is also largely marketed as a weight loss supplement, and claims to reduce levels of LDL cholesterol[65]. Although there have been many reports of beneficial effects, the açai berry is not yet listed on the U.S. Food and Drug Administration, Generally Recognized As Safe (GRAS) list. This is due to the limited available studies in the bioactivity of açai berry's constituents.

Açai berry has been shown to contain a variety of biologically active constituents such as hydroxybenzoic acids, antioxidant polyphenolics, flavon-3-ols, and anthocyanins[67]. Açai berry juice and pulp has also been examined by

another collaborating group here at UNCG, the Cech group. It was shown by their lab that the açai berry juice and pulp contains concentrations of anthocyanin – class flavonoids, namely cyanidin-3-O-glucoside (C3G) and cyanidin-3-O-rutinoside (C3R). After consumption of 18 fl. oz. açai berry juice, pharmacokinetic analysis of the oral bioavailability show that plasma anthocyanin concentrations reach a maximum of 1.1 – 2.3 ng/mL in an average adult. These compounds may be responsible for the antioxidant capabilities of açai berry, as they are capable of scavenging free – radicals[67]. In a study performed by Showande et al, a total monomeric anthocyanin value was determined in an ethanol extract of *Hibiscus sabdariffa*, which compared determined ratios of individual anthocyanin molecules in the extract to one another. These researchers showed an IC_{50} value of 306 µg/mL by the anthocyanins on CYP1A2 mediated metabolism[68]. This reported IC_{50} value is fairly high and physiologically irrelevant, which likely means that the anthocyanins found in the açai berry extracts will not have any effect on the CYP1A2 enzyme. Despite the somewhat related, previous work in this area, there have been no detailed studies investigating the effect of açai berry constituents on CYP450 detoxifying enzymes.

1.6.0 Bioassay – Guided Fractionation

One of the most common approaches to identifying active constituents in natural product research is a method termed bioassay guided fractionation (BGF). This process has shown great effectiveness in identifying medicinally active constituents from raw natural product material, as it evaluates the pharmacognostic properties of a crude plant extract, which contains an enormity of constituents. This method allows for the separation, isolation, and characterization of molecules within a crude mixture that may have physiological significance, whether medicinally or toxicologically, in the human body[69]. Paclitaxel, which is a very important chemotherapeutic used in the treatment of breast cancer, was discovered in this fashion from screening extracts of endophytic fungi found in the Pacific yew tree (*Taxus brevifolia*)[70].

1.7.0 Objective Statement

This project aims to investigate the inhibitory potential of the Amazonian açai berry (*Euterpe olecera*) on the Cytochrome P450 isoforms 1A1 and 1A2. Currently, there is no published literature demonstrating CYP450 inhibition by the açai berry. This project is part of a larger project aiming to investigate inhibition of all toxicological significant CYP450 isoforms. Research completed previously shows a modest inhibitory effect by açai berry extracts on isoforms 2E1, 2A6, and 3A4.

CHAPTER II

MATERIALS AND METHODS

2.1.0 Preparation of Bioassay Reagents

2.1.1 Potassium Phosphate Buffer

Separate 1 M solutions were prepared from crystalline monobasic and dibasic potassium phosphate, which were both purchased from Carolina Biological Supply Company. These solutions were combined to achieve a pH 7.4 buffer. This 1 M stock solution of potassium phosphate buffer was stored in a refrigerator, and was diluted to a concentration of 100 mM in reaction mixtures. Phosphate buffer (10 mM) was also used to dilute the cDNA expressed P450 isoforms, making them easier to handle during experiments.

2.1.2 NADPH

Nicotinamide adenine dinucleotide phosphate (NADPH), was obtained from Chem – Implex International Incorporated in the form of a tetrasodium salt. Nanopure water was used to dissolve the NADPH salt to create a 10 mM solution, which was partitioned into many smaller fractions. These stock solutions were kept frozen at -80°C until used in CYP450 assays.

2.1.3 CYP1A1 and CYP1A2 cDNA Expressed Isoforms

Specific CYP450 isozymes were acquired from Xenotech INC., and were utilized to provide greater certainty that the investigated isoform was solely

responsible for product generation. Upon arrival, enzymes were separated into 25 µL aliquots, which were stored at -80°C. Enzymes were removed from the freezer, thawed on ice, and diluted tenfold in 10 mM potassium phosphate buffer before the enzymatic assay to retain the enzyme's catalytic activity. Concentrations of enzyme used in each reaction varied with regard to the activity of the enzyme utilized in each experiment. Enzyme concentration in the purchased cDNA expressed CYP450 isoforms was listed at 1 µg/µL.

2.1.4 Preparation of 7EC Substrate Stock Solution

A selective substrate of CYP1A1 and CYP1A2 is 7-ethoxycoumarin (7EC), which was used to monitor product formation by the enzymes. Crystalline 7EC was purchased from Indofine Chemical Company LLC and was prepared as a concentrated, 20 mM stock solution and stored at ≈ -4°C, which was diluted to a concentration of 20 µM in each reaction unless otherwise stated. Since this molecule is fairly nonpolar it would not dissolve in water and had to be first dissolved in methanol prior to dilution with water. It is known that too high of a methanol concentration can inhibit enzymes, so to avoid this, the amount of methanol from the stock substrate was kept at 0.05% or lower in enzymatic reactions.

2.1.5 Açai Berry Extracts and Subsequent Fractionations

Freeze dried açai berry powder was obtained from Optimally Organic LLC. The crude plant material was extracted into four different initial solvents, by collaborators in Dr. Oberlies' research group. Samples received from the

Oberlies' lab were dissolved in solution and partitioned into smaller stock solutions, which were dried and refrigerated at 4°C with limited light exposure. Preparation of samples for use in CYP450 bioassays involved initial dissolution into methanol, which was diluted 100x with nanopure water. Keeping in mind that methanol concentrations may alter an enzymes activity, solvent controlled reactions were performed as part of the experiment to ensure enzymes were not affected by its presence. Concentrations of the açai berry extracts and fractions utilized in different experiments varied tremendously, ranging from 125 ng/mL to 200 µg/mL in reaction mixtures.

2.1.6 Preparation of Diosmetin Standard

Upon isolation of the compound diosmetin, it was of interest to test pure diosmetin in CYP450 enzymatic reactions. This compound was purchase from Indofine Chemical Company Incorporated. Crystalline diosmetin was initially dissolved in 100% DMSO, and diluted with nanopure water accordingly to the necessary concentrations needed for reactions.

2.2.0 Cytochrome P450 Assays

A common approach used to investigate enzyme activity is to use an *in vitro* enzymatic bioassay to measure product formation resulting from catalysis. Each bioassay consisted of a series of enzymatic reaction mixtures containing either CYP1A1 or 1A2 isozyme, phosphate buffer (pH 7.4), 7EC substrate, NADPH, and nanopure water to dilute all mixtures to a constant 200 µL volume. To ensure that the enzyme was working at its full capability, parameters were

evaluated in terms of enzyme concentration and incubation time. Product formation appears to respond linearly when enzyme concentration, and incubation times were varied, and the pertaining data can be found in sections 3.1.1 and 3.1.2 of the results and discussion chapter.

2.2.1 CYP1A1 Model Assay

An *in vitro* model of CYP1A1 enzyme reactions was achieved by utilizing cDNA expressed CYP450 isoforms, and its proposed mechanism is shown in Figure 8. This method allows for the quantification of only products formed via CYP1A1 catalysis, which yields more significant, meaningful data. CYP1A1 is largely a metabolizer of endogenous substrates, such as melatonin and arachidonic acid[26]. A commonly used substrate to investigate CYP1 reactions is 7-ethoxycoumarin, which is a known anticoagulant. CYP2 and CYP3 families have also been shown to be active catalysts for oxidation of this substrate[71]. However, since only the CYP1A1 isoform is being used, results cannot be skewed by product formation from other metabolizers. The substrate molecule, 7-ethoxycoumarin, undergoes O-deethylation by CYP1A1 enzymes, which results in the production of 7-hydroxycoumarin, more commonly known as umbelliferone, along with acetaldehyde.

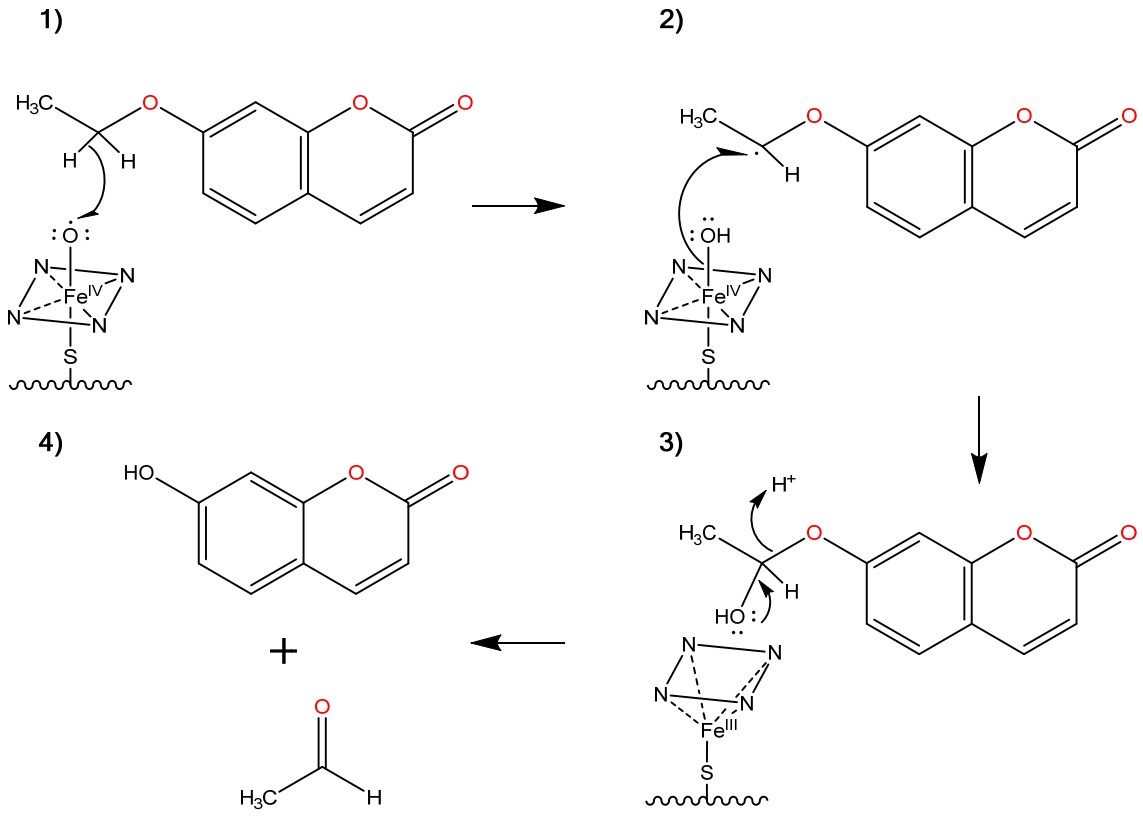

Figure 8. Proposed Mechanism for CYP1A1 O-Deethylation. Steps showing the hydrogen abstraction and oxygen rebound, which result in product 7-hydroxycoumarin and acetaldehyde.

This assay was carried out in 1.5 µL centrifuge tubes containing 20 µM 7-ethoxycoumarin , 100 mM potassium phosphate buffer (pH 7.4), 1 mM NADPH, and cDNA expressed CYP1A1 enzymes (5 uµ/mL), in a constant reaction volume of 200 µL. Reactions were initiated upon the addition of NADPH, and incubated at 37°C for ten minutes. After ten minutes, reactions were quenched with 25 µL of 70% perchloric acid, and placed on ice to precipitate proteins. Samples were then centrifuged at 15,800 g for eight minutes, and the supernatant was

extracted for analysis. The supernatant was analyzed using HPLC UV/vis detection at a wavelength of 320 nm.

2.2.2 CYP1A2 Model Assay

Assays performed to investigate CYP1A2 enzyme activity were very similar to the previously mentioned CYP1A1 assays. As 7-ethoxycoumarin is a widely used substrate probe for CYP1 family reactions, this substrate was also utilized for CYP1A2 assays[71]. However, it was found that this isoform did not catalyze the commonly observed O-deethylation reaction seen in other isoforms, and the corresponding mechanism is shown in Figure 9. Instead, it was observed that a molecule that eluted later than 7-hydroxycoumarin was the major metabolite of the CYP1A2 enzymatic reaction. Due to the increased retention time of this compound, it is believed that CYP1A2 catalyzes an epoxidation reaction somewhere on the bicyclic, aromatic ring. However, it is not known exactly where this epoxidation is taking place.

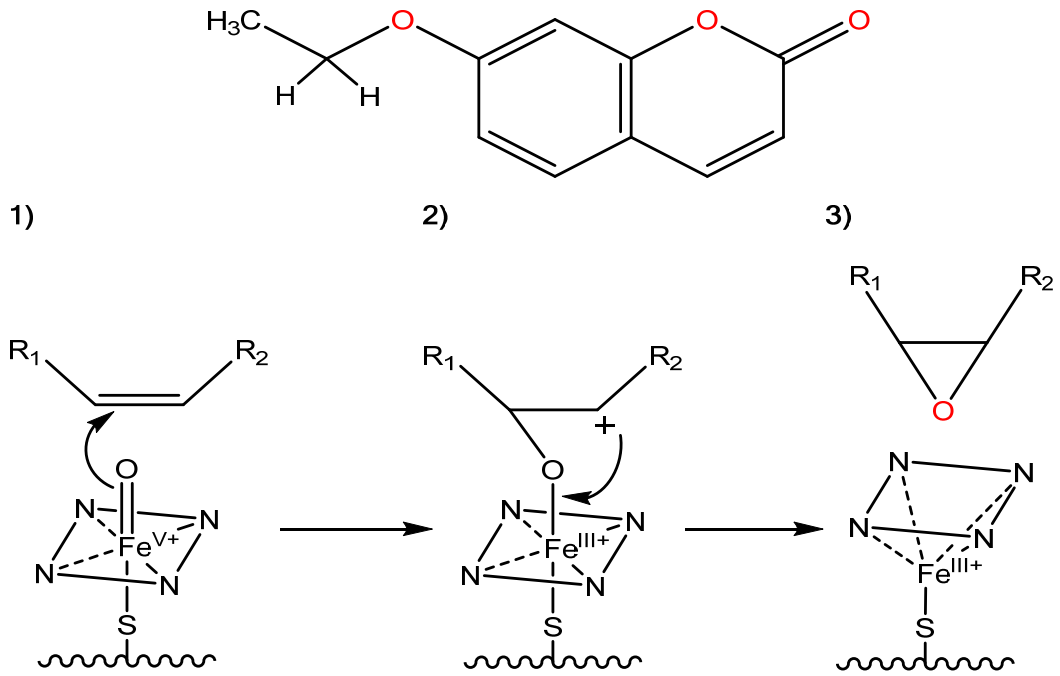

Figure 9. Proposed Mechanism of CYP1A2 Epoxidation. Due to a more hydrophobic molecule observed in 1A2 reactions, an epoxidation is thought to be occurring.

Enzymatic assays for this isoform were carried out in 1.5 µL centrifuge tubes containing 20 µM 7-ethoxycoumarin, 100 mM potassium phosphate buffer (pH 7.4), 1 mM NADPH, and cDNA expressed CYP1A2 enzymes (12.5 µg/mL), in a constant reaction volume of 200 µL. Addition of NADPH was used to initiate the reactions, and reactions were incubated at 37°C for ten minutes. Termination of reactions was accomplished by the addition of 25 µL of 70% perchloric acid. Samples were immediately placed on ice to precipitate the protein, and spun at 15,800 g to separate the supernatant from the precipitant. The supernatant was extracted for HPLC UV/vis detection at 320 nm.

2.2.3 High Performance Liquid Chromatography (HPLC)

HPLC analysis was performed using a Shimadzu LC-20AT, with a UV/vis PDA detector. Analysis of the product 7-hydroxycoumarin molecule was carried out using an isocratic mobile phase that consisted of 60% nanopure water, 40% acetonitrile, and 0.1% trifluoroacetic acid, and an extended C18 column for the stationary phase. The product showed UV absorbance at 320 nm and a retention time of about 3.5 minutes[71, 72]. Chromatogram run times were set to ten minutes, with the product eluting at about 3.5 minutes and the substrate eluting at about 6 to 7 minutes. Generated product peaks were integrated and used to analyze data.

2.2.4 Data Analysis

From the chromatograms that were generated by HPLC analysis, the retention time of the product 7-hydroxycoumarin was determined, and the corresponding peak was integrated and its area was quantified using the Shimadzu computer software. Acquired peak areas were given arbitrary units and are a representation of the assayed enzyme's activity. Assays were performed in duplicates unless otherwise stated and the reported enzyme activity reflects the average of that specified test group.

2.3.0 Extraction of Açai Berry Powder

Solvent portioning was used to create four crude açai berry extracts, from the freeze dried açai berry plant material. This process, which is described in Scheme 1, involved the initial dissolution of the crude plant material into a 10:1:9

hexane:water:methanol mixture. Using a separatory funnel, the organic layer was extracted from the mixture, which isolated highly lipophilic components, such as fatty acids and oils. This isolate was rationed into smaller samples and dried to produce the hexane extracts. The remaining aqueous methanol layer was mixed with chloroform to yield a 4:1:5 chloroform:water:methanol mixture. Once again, the organic phase was extracted, rationed, and dried to generate the chloroform extracts. Addition of butanol to the remaining aqueous phase created a 1:1 butanol:water mixture. Both the butanol and aqueous phases were collected separately, rationed, and dried to create the aqueous and butanol extracts.

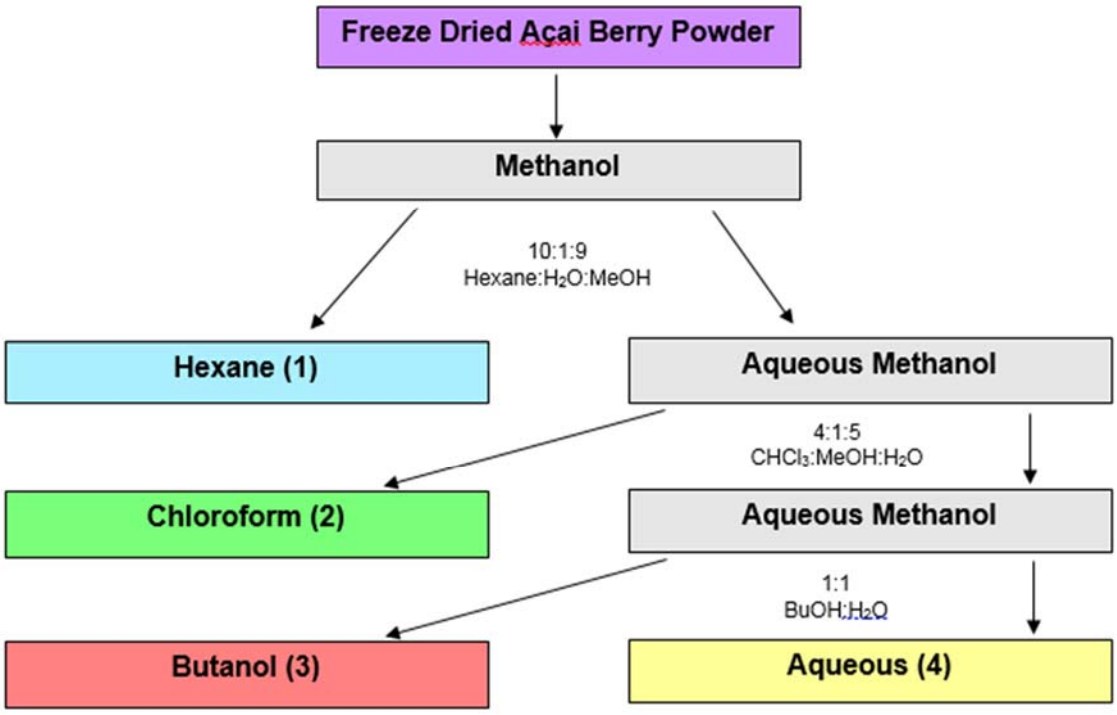

Scheme 1. Flow Diagram of Açai Berry Extraction. Yielded four different extracts depending on solvent used.

2.3.1 Fractionation of Açai Berry Extracts

A diagram depicting the entire fractionation process throughout this process can be found below in Scheme 2. As described in the previous section, four different extracts were generated from the freeze dried açai berry plant material. Fractionation of these extracts was performed by our collaborators in the Oberlies' laboratory, at UNCG. Fractionation of the chloroform extract was accomplished with silica-column flash chromatography (RF CombiFlash) using a hexane:chloroform:methanol solvent gradient to generate the 34-series fractions. Sample 34-8 was selected to be further investigated, and was separated using

the same instrument, but used a solvent gradient of hexane:acetone to generate the 38-series fractions. Separation of fraction 38-3 was accomplished using a diol column and a solvent gradient of 100% hexane, to 100% ethylacetate, to a 1:4 ethylacetate:water solution, which created the series termed the 63-series fractions. Fraction 63-4 was chosen for further fractionation using reverse phase chromatography with an ISCO C18 column, and a solvent gradient of 1:9 methanol:water to 100% methanol. Separation of fraction 63-4 generated the 94-series fractions, which were high in purity.

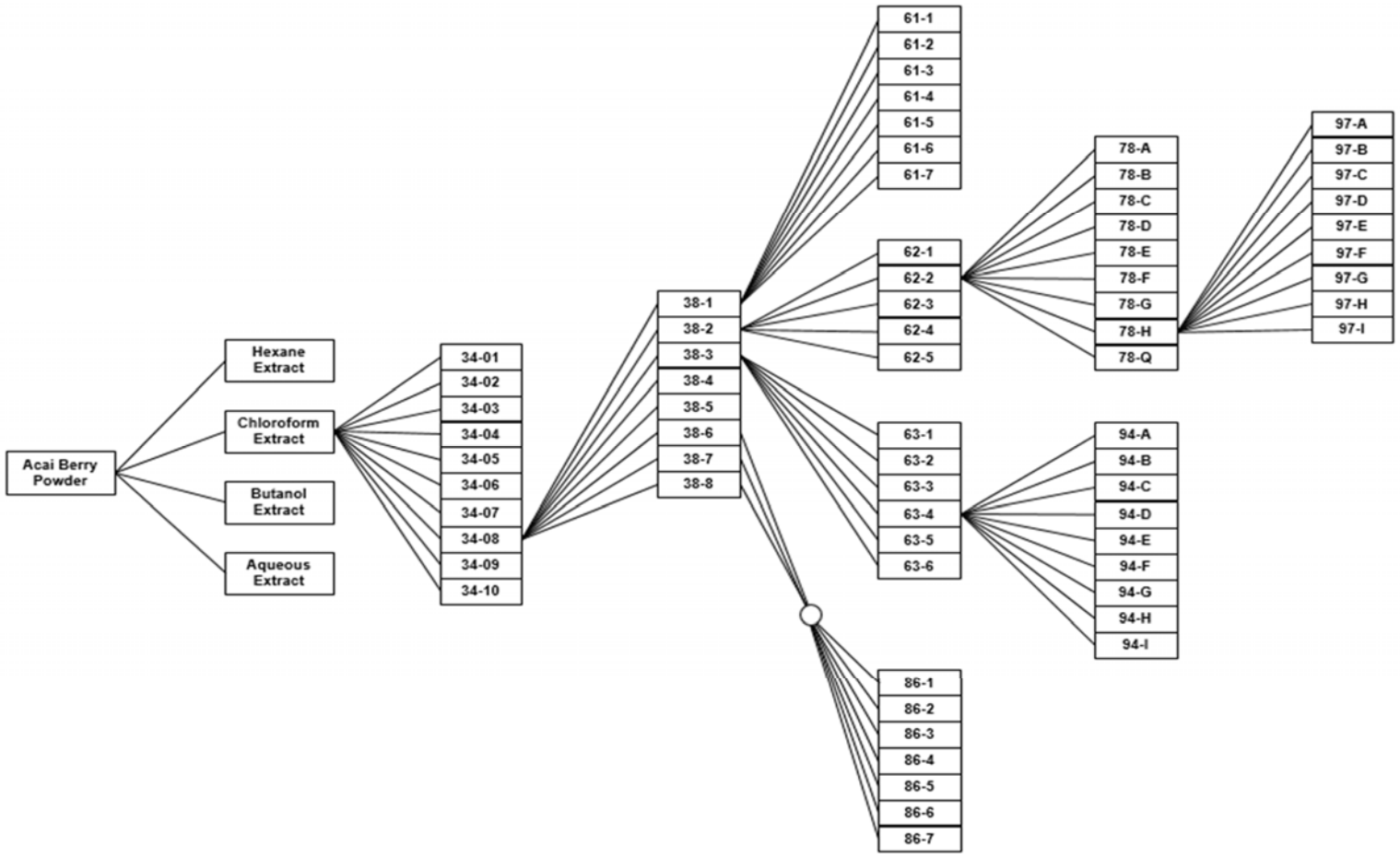

Scheme 2. Flow Diagram Depicting Entire Bioassay Guided Fractionation of Açai Berry Extract. This scheme corresponds to data collected from CYP1A1 enzymatic reactions

CHAPTER III

RESULTS AND DISCUSSION

3.1.0 Bioassay Development

In order to measure activities of CYP450 isoforms 1A1 and 1A2, several components of each assay were tested in variable quantities. To optimize these assays, variables such as enzyme concentration and incubation time were examined. A linear trend should be observed with increasing incubation time and enzyme concentration. These parameters were investigated to ensure that each CYP450 reaction followed typical enzymatic behavior, and to optimize the utilized assay prior to the açai berry inhibition screening.

3.1.1 CYP1A1 Model Assay

The enzyme reaction using CYP1A1 enzymes was first tested in respect to varying incubation times. It was the goal of this experiment to establish linearity between the enzyme's activity and the time allotted for reactions to incubate, as well as determine the optimum time for each performed enzyme reaction. These reactions were performed as described in the previous section. Below in Figure 10, a graph can be found displaying the results from this assay. Incubation time was varied from 0.0 minutes, to 5.0 minutes, to 10.0 minutes, and to 30.0 minutes, and reported activities were measured in arbitrary activity units (AU). A linear trend was observed from 0.0 minutes to 10.0 minutes, with

the observed activity at 30 minutes appearing to deviate slightly from the linear trend. This is most likely due to a decrease of enzymatic activity from an increased exposure to heating, or a decrease in adequate substrate concentrations. From data collected at 0.0, 5.0, and 10.0 minutes, an R^2 value of 0.9992 was calculated. It was decided to use an incubation time of ten minutes per each enzyme assay.

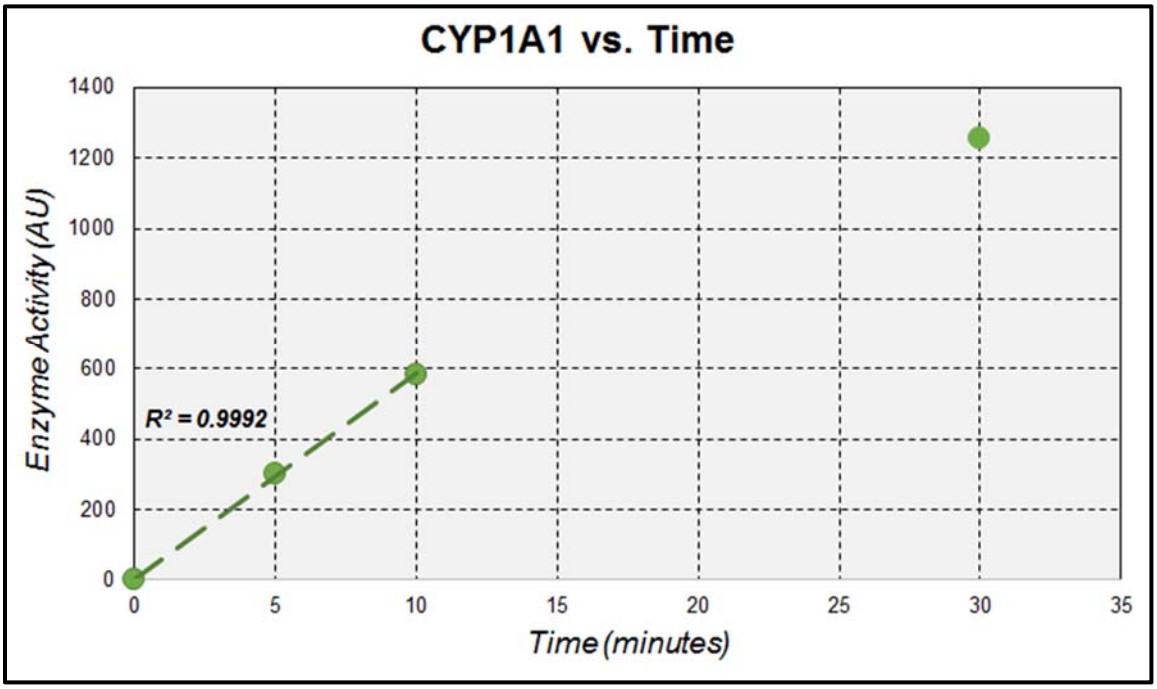

Figure 10. Results Observed from Variation of Incubation Time Using CYP1A1.

Examining the effect of increasing enzyme concentrations was also of interest to ensure the assay was working properly, as well as to choose an optimum concentration to be used in each assay. An optimum concentration would produce an activity that was sufficient enough to quantitate, keeping in mind that during inhibition studies the activity would decrease, but to also be low enough to conserve the purchased cDNA expressed enzymes. Linearity was established between enzyme volume and enzymatic activity, which can be seen in Figure 11. Enzyme concentrations of 0.0 µg/mL, 0.5 µg/mL, 1.0 µg/mL, and 5.0 µg/mL were tested, and each reaction was incubated for ten minutes. Enzymatic activity was measured in arbitrary activity units (AU), and it was determined that this data fit a linear trend with a R^2 value of 0.9998. It was also determined that using a volume of 1 µL of cDNA expressed 1A1 enzymes would be sufficient for each reaction.

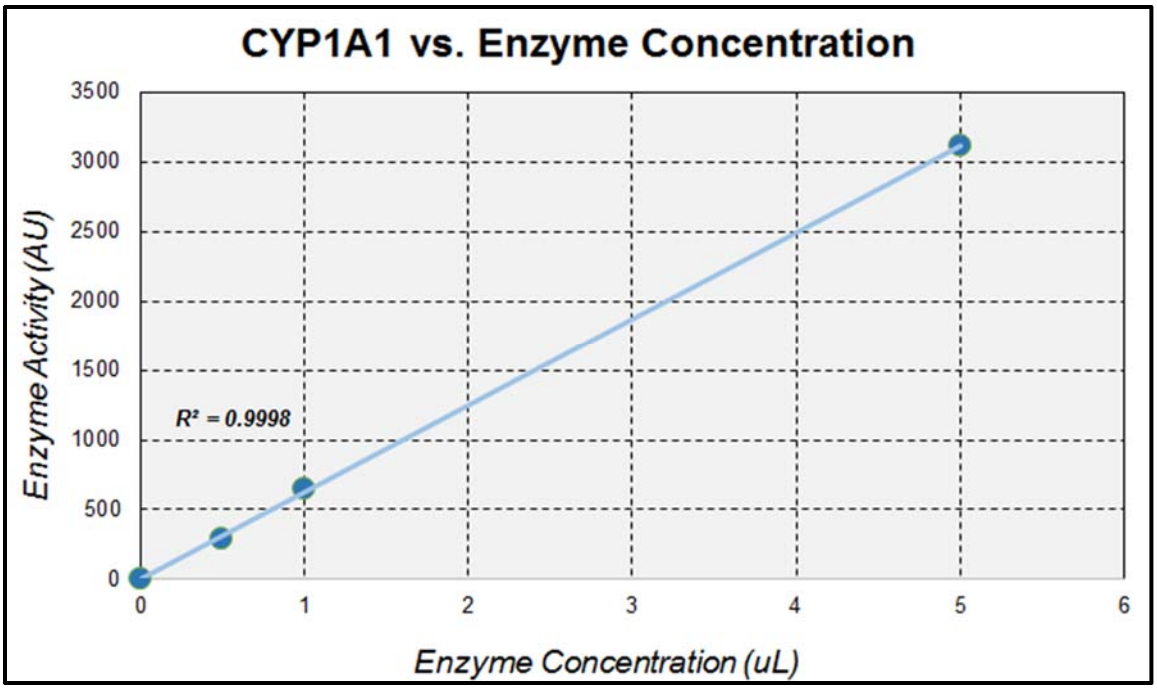

Figure 11. Results for Variation of Enzyme Concentration With CYP1A1.

3.1.2 CYP1A2 Model Assay

Enzyme reactions using the CYP1A2 were also tested with various incubation times. A linear trend should be observed between an enzyme's activity and incubation time while the enzyme is most active. It was known that too long of an incubation time would cause a decrease in activity, due to denaturation or a decrease in substrate availability. Incubation times were varied from 0.0 minutes to 30.0 minutes, and all reaction mixtures were made identical to one another. Results from this experiment were measured in arbitrary activity units (AU), and can be found in Figure 12. Observed data showed a linear trend from times 0.0 minutes to 10.0 minutes, with a calculated R^2 value of 0.9998. At 30.0 minutes the observed activity appeared to deviate from linearity as

expected. As with the CYP1A1 isoform, it was decided that an incubation time of 10.0 minutes would be an optimum time.

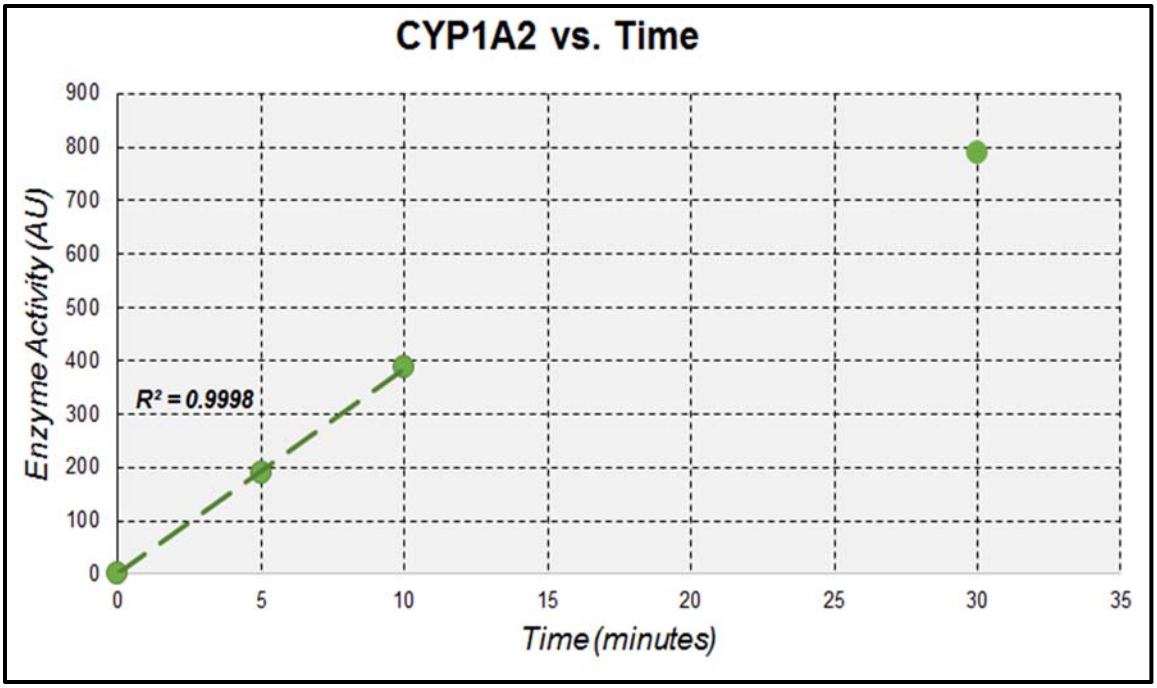

Figure 12. Results for Variation of Incubation Times Using the CYP1A2 Isoform.

Effect of increasing cDNA expressed enzyme concentration was also examined to ensure enzymes were working properly, and to also choose an optimum volume per reaction. An increasing enzyme concentration should directly correlate with the observed enzyme activity. Results from this experiment are shown in Figure 13, and varied enzyme concentrations from 0.0 to 10.0 µg/mL. Each reaction was allotted an incubation time of ten minutes. A linear trend was established for this data set, with a R^2 value of 0.9999. It was decided to use an enzyme volume of 2.5 µL for each CYP1A2 assay.

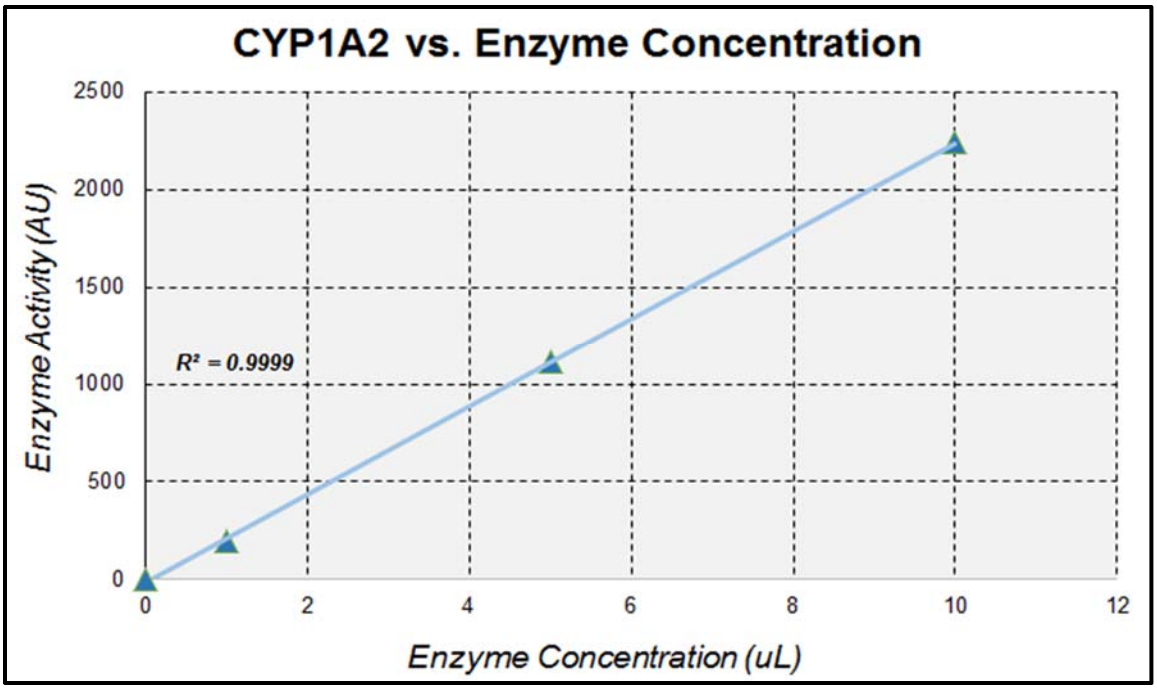

Figure 13. Results for Variation of Enzyme Concentration Using the CYP1A2 Isoform.

3.2.0 Bioassay – Guided Fractionation of Açai Berry

Initial fractionation of the açai berry, which is summarized in scheme 1, produced four crude extracts that were tested in CYP450 assays. These crude extracts were tested in CYP1A1 and CYP1A2 enzyme reactions, as described in the Materials and Methods section. Observed results were as follows:

3.2.1 CYP1A2 versus Crude Açai Berry Extracts

The four initial, crude extracts were assayed in enzymatic reactions using CYP1A2 enzymes. Crude aqueous, butanol, hexane, and chloroform extracts were screened in bioassays utilizing the 1A2 isoform. Extracts were each evaluated at varied dosages of 10, 25, 50, and 100 µg/mL, to examine possible

interactions between an extract and the enzyme. Collected data from screening CYP1A2 in the presence of the crude açai berry extracts can be found below in Figure 14.

When the aqueous extract was tested in CYP1A2 enzyme reaction, minimal inhibition was observed. At concentrations of 10 and 25 µg/mL there was no inhibition observed. At an increased concentration of 50 µg/mL an inhibition value of 2.71% was observed, and at an extremely high concentration of 100 µg/mL a slightly more modest value of 29.2% was observed.

An assay was performed to examine the effect of the crude butanol extract on CYP1A2 activity. This extract showed no inhibitory effect on CYP1A2 at concentrations of 10, 25, and 50 µg/mL. Even when tested at a concentration of 100 µg/mL, only an inhibition value of 12.5% was observed.

Surprisingly, when the crude chloroform extract, which was hypothesized to exert the most potent inhibitory effects, was tested in CYP1A2 enzymatic assays, little effect was observed. At extract concentrations of 10, 25, and 50 µg/mL, there was no inhibition observed. An inhibition value of 20.4% was reported when the extract was assayed at 100 µg/mL.

Of all the crude extracts evaluated in regards to CYP1A2 activity, the hexane extract proved to show the most potent inhibitory effect. Although at a concentration of 10 µg/mL there was no observed inhibition, at a concentration of 25 µg/mL an inhibition value of 8.27% was shown, at a concentration of 50 µg/mL a value of 50.2% was shown, and at a concentration of 100 µg/mL a value

of 96.0% was shown. From the data collected from this bioassay, an IC_{50} value between 49.0 – 50.0 µg/mL can be estimated for the hexane extract. Despite the hexane extract proving to be the most potent inhibitor for the CYP1A2 isoform, chromatographic separation of lipid-like molecules often collected from hexane extractions is usually very difficult. For this reason the hexane extract was not further purified and examined.

Data collected from screening CYP1A2 against the crude açai berry extracts showed no inhibitory effect at the lowest tested dosage of 10 µg/mL for any of the extracts. At a dosage of 25 µg/mL the hexane extract showed a weak inhibition value of 8.27%, and was the only extract to have any effect. Only at the highest tested concentration of 100 µg/mL was inhibition observed for all extracts. Because of the poor results gathered from CYP1A2 assays with the crude extracts, it was decided to discontinue work with this isoform, and shift the focus towards the related CYP1A1 isoform.

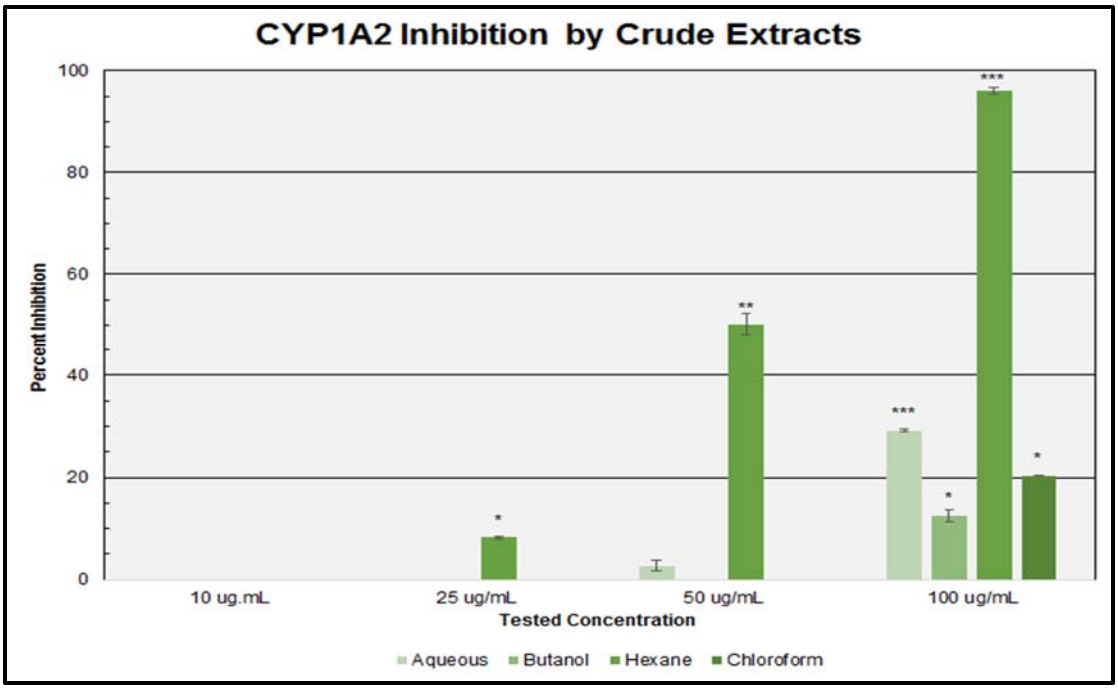

Figure 14. Inhibitory Effect of Crude Açai Berry Extracts on CYP1A2.

3.2.2 CYP1A1 versus Crude Açai Berry Extracts

Crude extracts that were tested in CYP1A2 reactions, were also tested in CYP1A1 reactions. Dose dependent bioassays were performed with the crude aqueous, butanol, hexane, and chloroform extracts, at dosages of 10, 25, 50, and 200 µg/mL, unless otherwise stated. Results gathered from examining the effects of the crude açai berry extracts on CYP1A1 may be seen below in Figure 15.

CYP1A1 enzymatic reactions were carried out in the presence of increasing dosages of the aqueous extract, and showed little inhibition. Observed inhibition was only 4.72% at 10 µg/mL, 3.92% at 25 µg/mL, 15.3% at 50 µg/mL, and 40.6% at 200 µg/mL. The low observed inhibition is most likely

due the fact that water soluble components of plants, such as some vitamins and other nutrients, rarely come into contact with the CYP450 enzymes. Water soluble compounds that enter the body are usually taken up in the stomach to be used elsewhere in the body or are passed along to the intestinal tract for riddance from the body or further reabsorption[5].

Reactions were performed using incremental dosages of the butanol extract. Observed inhibitions were 31.5% at 10 µg/mL, 74.5% at 25 µg/mL, and 88.6% at 50 µg/mL. Reactions were also carried out using 200 µg/mL, but the generated data was not quantifiable due to positive interference from constituents in the butanol extract, which eluted at the same time. Although a fairly high inhibition value was seen at high dosages, they are somewhat insignificant because these concentrations are much too high compared to what would be seen in a physiological system.

When reactions were tested in the presence of an increasing hexane extract concentration, observed inhibition was 51.4% at 10 µg/mL, 73.0% at 25 µg/mL, 80.4% at 50 µg/mL, and 52.7% at 200 µg/mL. At a dosage of 200 µg/mL the acquired inhibition value (52.7%), was lower than the value (80.4%) obtained at 50 µg/mL. This may indicate a mode of non-competitive inhibition, a way in which the inhibiting component does not compete with the actual substrate (7-ethoxycoumarin) for a place in the active site of the enzyme. Despite displaying promising values of inhibition at lower extract concentrations, as well as interesting results at higher concentrations, the hexane extract was not further

separated. This is because hexane is a nonpolar solvent and typically extracts lipid or lipid-like molecules, which can prove to be quite challenging to separate via preparative chromatography.

As expected, the chloroform extract proved to be the most potent inhibitor at low concentrations. According to the data obtained from a dose dependent bioassay examining the chloroform extract, inhibition values were 79.2% at 10 µg/mL, 89.4% at 25 µg/mL, 94.8% at 50 µg/mL, and 97.9% at 200 µg/mL concentrations. The collected data appears to demonstrate a sigmoidal curve, which is characteristic of testing inhibitors at incremental concentrations.

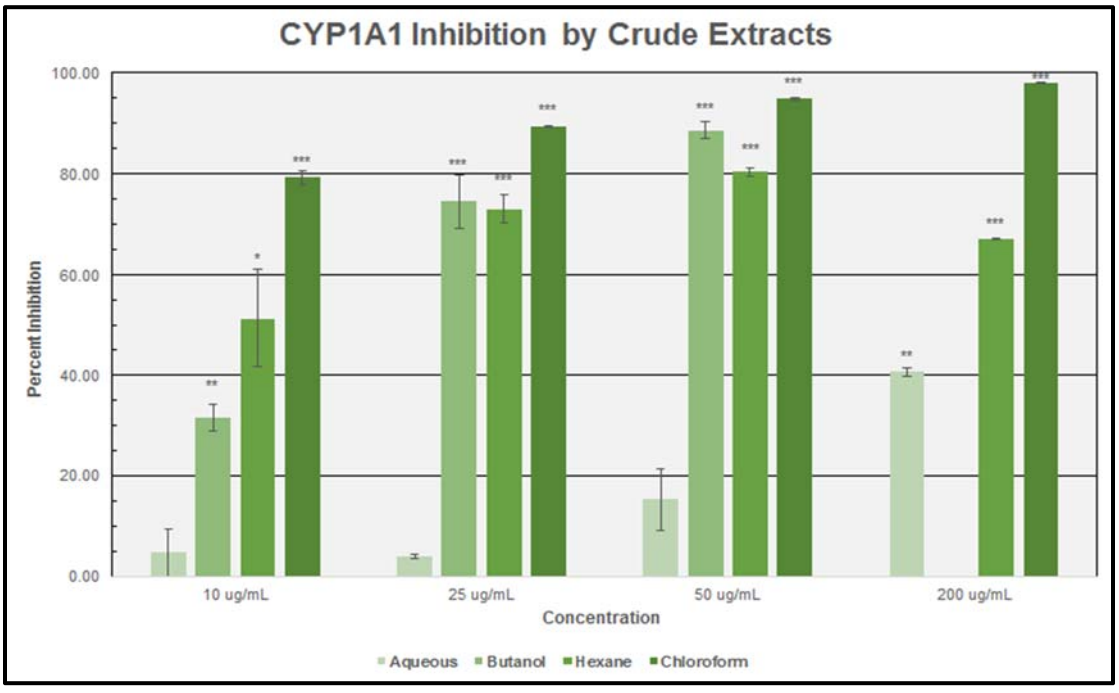

Figure 15. Inhibitory Effect of Crude Açai Berry Extracts on CYP1A1.

An assay was performed to evaluate kinetic parameters of the CYP1A1 enzyme in the presence of the crude chloroform extract. A Michealis – Menten plot of this data can be seen below in Figure 16. This was accomplished by preparing reaction mixtures with varied substrate concentrations, containing either no inhibitor, or inhibitor kept at a constant concentration. Observed enzyme activity, for both the inhibited and non – inhibited samples, was plotted versus its associated substrate concentration. Using the Michealis – Menten model of enzyme kinetics, a curve was generated to fit both sets of collected data. From these curves it was shown that in the presence of no inhibitor CYP1A1 enzymes had a K_m of 18.9 ± 4.95 μM and a V_{max} of 1150 AU. In the presence of 2 μg/mL of crude chloroform extract a K_m of 49.6 ± 10.9 and a V_{max} of 1148.0 AU, while increasing the inhibitor concentration to 5 μg/mL results showed a K_m of 69.6 ± 16.2 μM and a V_{max} of 1778.2 AU. Due to the apparent competitive nature of this inhibitor, the V_{max} was set to a constant 1125 AU in the Michealis – Menten equation used to fit the data. Using the equations mentioned previously in section 1.3.1, a K_i was calculated from results at both inhibitor concentrations. At a 2 μg/mL inhibitor concentration the calculated K_i was 1.23 ± 0.30 μg/mL, and at an inhibitor concentration of 5 μg/mL the resulting K_i was 1.86 ± 0.46 μg/mL.

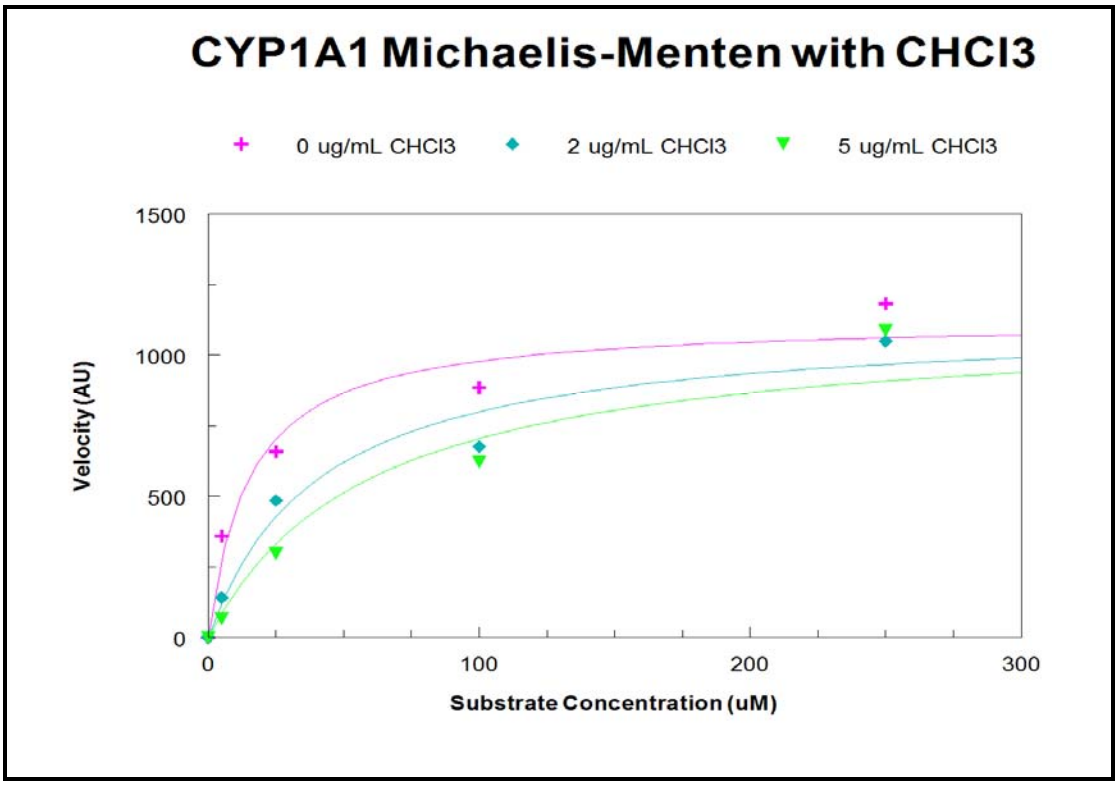

Figure 16. Michealis – Menten Plot of CYP1A1 in the Presence of Crude Chloroform Extract.

3.2.3 The 34- and 38-Series Compounds

Fractionation of the chloroform extract yielded the samples deemed the 34-series, which contained ten fractions, labeled from 34-1 to 34-10. A graph depicting results from screening the 34-series at 20 µg/mL can be found directly below this paragraph in Figure 17. When reactions were carried out using a concentration of 20 µg/mL of the specific fraction, inhibition values were 60.6% for 34-1, 58.8% for 34-2, 37.3% for 34-3, 23.6% for 34-4, 42.7% for 34-5, 37.5% for 34-6, 55.5% for 34-7, 73.3% for 34-8, 25.2% for 34-9, and 45.6% for 34-10. It was shown that among the 34-series that the 34-8 fraction displayed the most

potent inhibition at 73.3%, and the least potent inhibition was observed with the 34-4 fraction at 23.6%. The crude chloroform extract was also tested with this series and showed an inhibition value of 65.4%, which was slightly lower than the 34-8 fraction. Due to such high inhibition portrayed by the 34-8 fraction, this fraction was chosen for further separation.

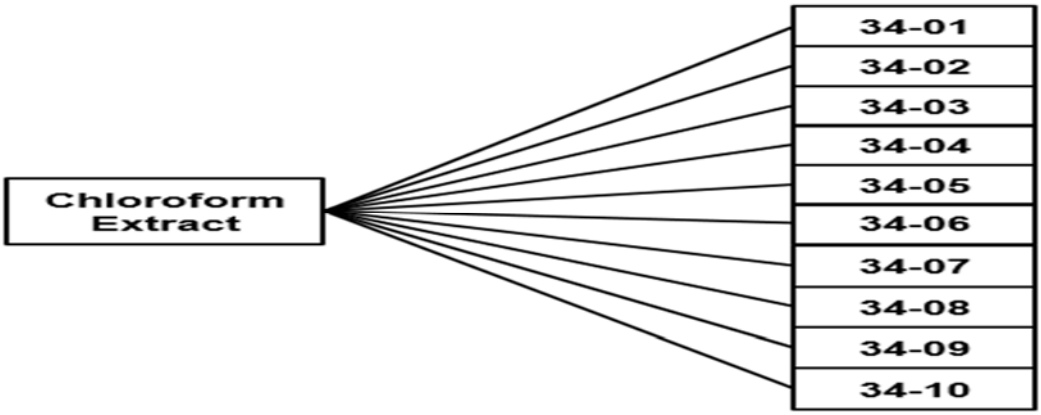

Scheme 3. Fractionation of Chloroform Extract into the 34-series Fractions.

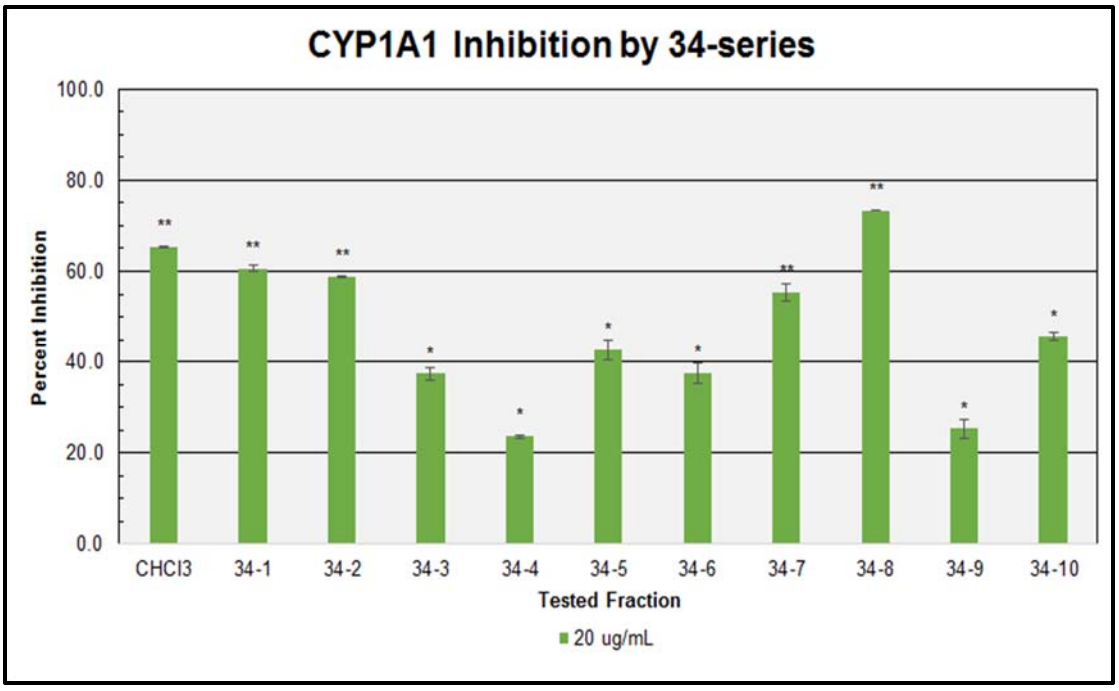

Figure 17. Screening of the 34-series Fractions on CYP1A1.

The 34-8 fraction was separated into a new series termed the 38-series, which originally consisted of eight different fractions. Fractionation of 34-8 resulted in acquiring minimal amounts of samples 38-6, 38-7, and 38-8, which were re-pooled and subjected to the fractionation process again to yield the 86-series mentioned later in this chapter, which can be found in Figure 26. Results gathered from screening the 38-series at a 20 µg/mL is displayed below in Figure 18. Remaining samples in the 38-series were tested in enzyme reactions at 20 µg/mL and displayed inhibition values of 63.7% for 38-1, 72.3% for 38-2, 78.0% for 38-3, 41.3% for 38-4, and 43.1% for 38-5. Fraction 38-3 showed slightly higher inhibition than its parent fraction 34-8, which was screened alongside the 38-series in the same assay and showed an inhibition value of 76.3%. Although

fraction 38-1 (63.7%), and 38-2 (72.3%), showed slightly lower inhibition values than their parent fraction 34-8, assays were further conducted containing their subsequently fractionated series. Separation of 38-1 yielded the 61-series, while 38-2 yielded the 62-series, and 38-3 yielded the 63-series. Data collected from screening these series at 20 μg/mL showed a similar pattern as to what was observed from screening the 38-series, with many individual fractions displaying inhibition values greater than 50%.

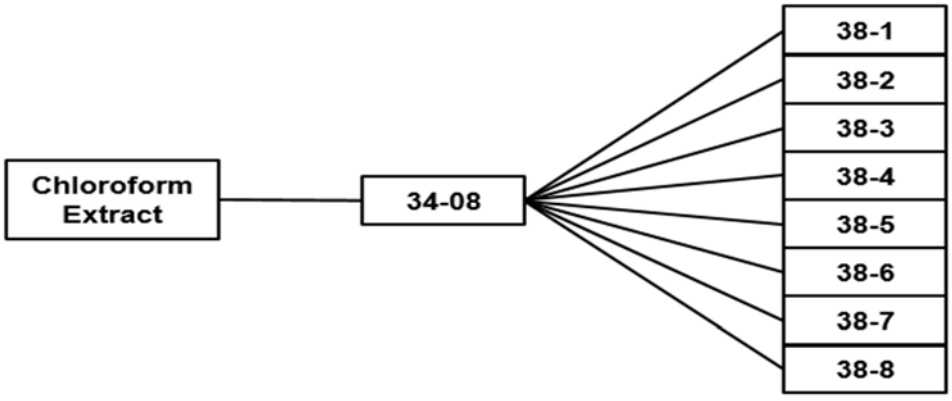

Scheme 4. Generation of the 38-series Fractions from Parent Fraction 34-08.

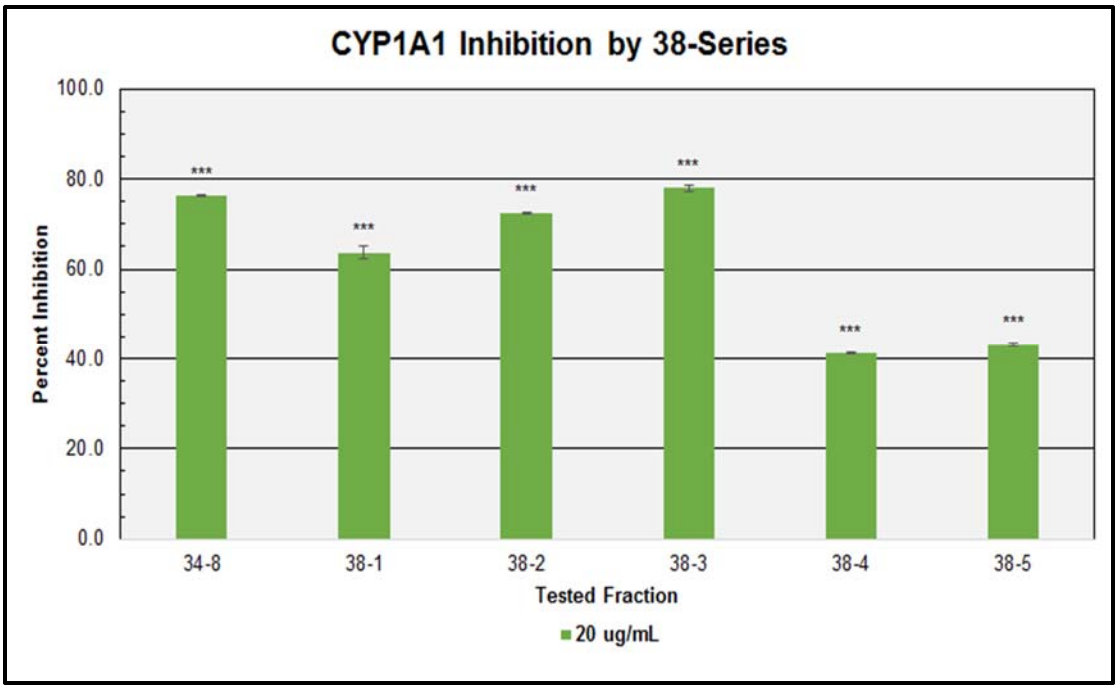

Figure 18. Screening of the 38-series Fractions on CYP1A1.

It was also decided at this point to approach this project using three different variations of bioassay – guided screening. The first approach involved testing a series of later stage fractions, the 97-series, which had been already separated for previous projects using different isoforms. If inhibition was observed in the 97-series, it was also of interest to trace the inhibition back to the 62-series. Second, it was of interest to test the 86-series fractions as the parent fractions 38-6,7,8 had not been previously screened. Continuation of the original bioassay – guided fractionation scheme at lower, more significant concentrations was the final approach.

3.2.4 Backtracking Inhibition from 97-Series Compounds

Another project tracking inhibition with the isoform CYP2E1, lead to the 97-series fractions, which are subsequent fractionations of the 62-2 fraction. It was also known that this series contained fractions consisting of pure compounds, which justified the deviation from the usual bioassay – guided approach. To ensure that inhibition would be observed, this series was screened at relatively high concentrations. A graph containing data from the 97-series assay is shown in Figure 19. When screened at a concentration of 20 µg/mL the inhibition value was 73.2% for 97-A, was 70.2% for 97-B, was 73.1% for 97-C, was 71.6% for 97-D, was 74.8% for 97-E, was 61.1% for 97-F, was 61.7% for 97-G, was 65.0% for 97-H, and was 68.0% for 97-I.

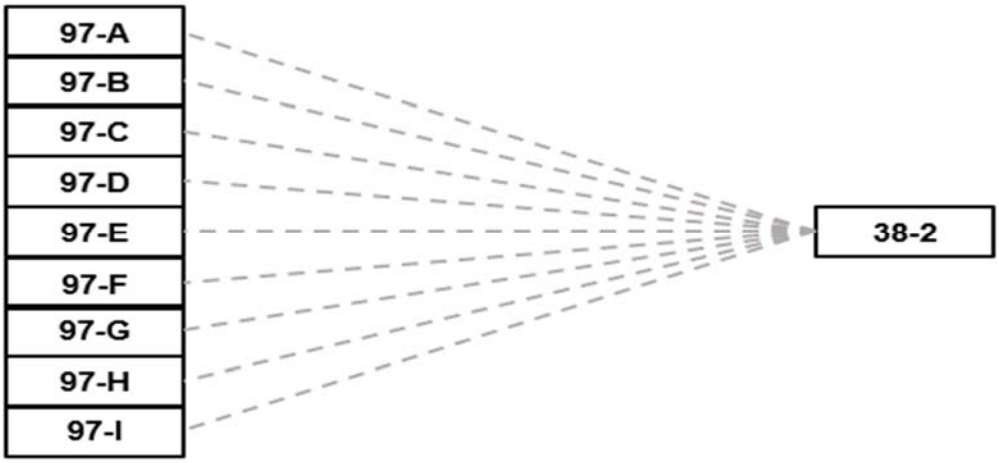

Scheme 5. Backtracking of the 97-series Fractions to Fraction 38-2. Fraction 38-2 is a crude fraction in which the 97-series was originally contained.

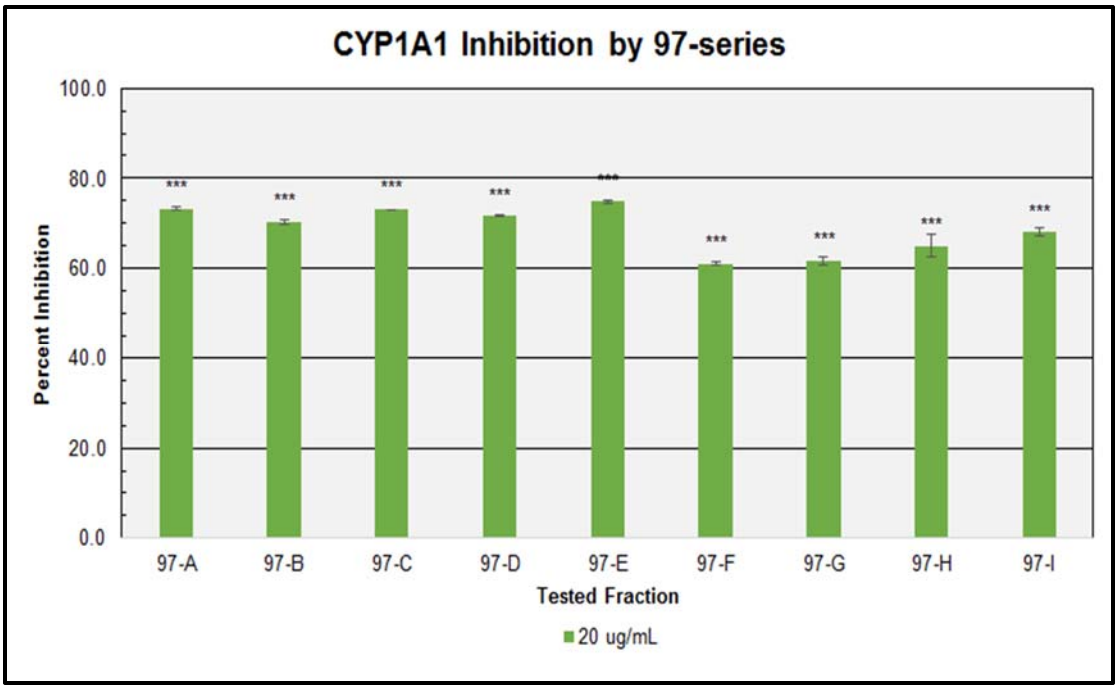

Figure 19. Screening of the 97-series Fractions on CYP1A1.

Fractions 97-B and 97-D were largely a single compound, and these fractions were further purified for identification by collaborators in the Oberlies laboratory. Structure elucidation of these fractions showed that both were phaeophorbide molecules, and differed in the alkylation of an ester moiety. Figures 20 and 22 show the elucidated structures of fractions 97-B and 97-D. It was of interest to test the dose-dependent effect of both of these fractions. Results observed from assaying CYP1A1 in incremental amounts of fractions 97-B can be seen below in Figure 21, while directly below in Figure 23 data from 97-D is shown. Both fractions were tested at incremental doses of 1, 5, 10, and 20 µg/mL. Observed results for 97-B at 1 µg/mL was 26.3%, at 5 µg/mL was 59.4%, at 10 µg/mL was 67.0%, and at 20 µg/mL was 74.2%; while for 97-D at 1 µg/mL

was 31.8%, at 5 µg/mL was 61.1%, at 10 µg/mL was 69.8, and at 20 µg/mL was 73.2%. Although inhibition values observed from both fractions at doses of 5, 10, and 20 µg/mL appear rather high, they are not very significant, as both fractions are relatively pure and a bioavailability at these concentrations in a physiological system is not attainable. More interest is focus on results gathered at a dose of 1 µg/mL, as even though it is still rather high for a physiological setting, it is still a more realistic concentration. Inhibition values of 26.3% for 97-B and 31.8% for 97-D, indicate that these phaeophorbide molecules are a slightly mild inhibitor of CYP1A1.

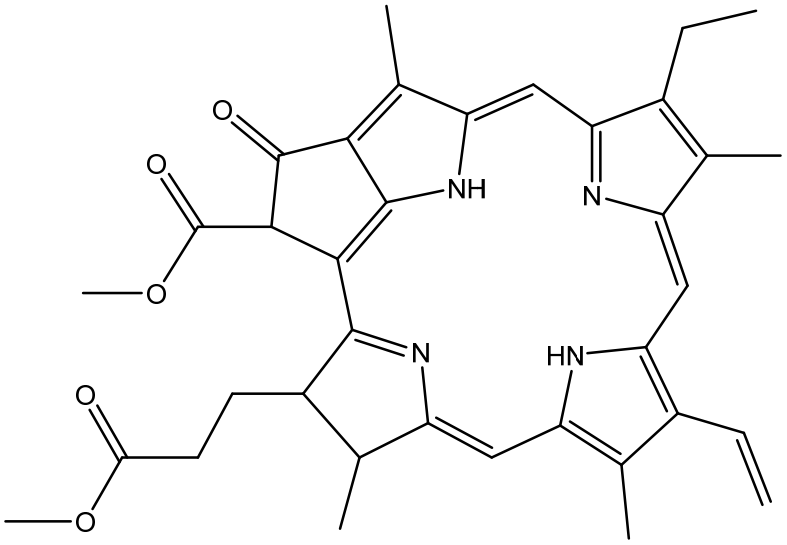

Figure 20. Elucidated Structure of Fraction 97-B. It was found to be a phaeophorbide molecule containing a methyl ester at the 3'' position.

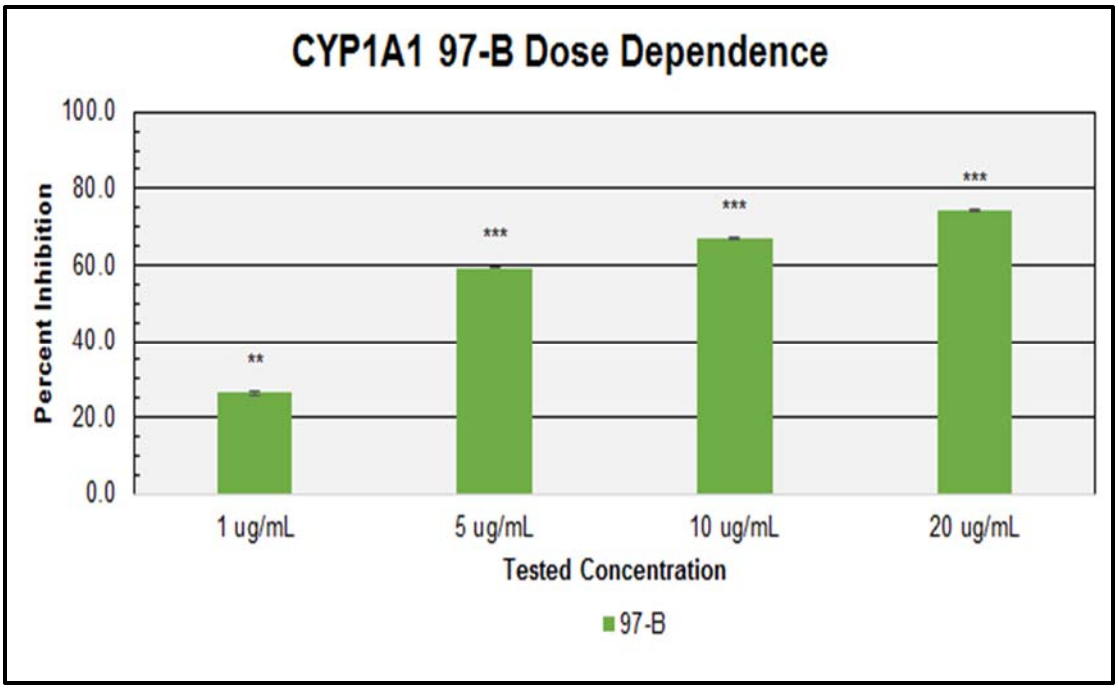

Figure 21. Effect of Incremental Concentrations of Fraction 97-B on CYP1A1.

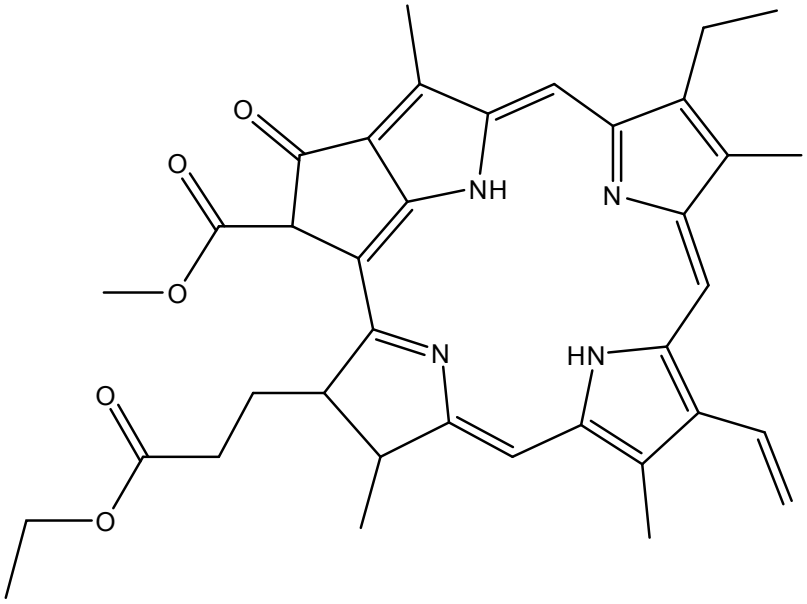

Figure 22. Elucidated Structure of Fraction 97-D. It was found to be a phaeophorbide molecule containing an ethyl ester at the 3'' position.

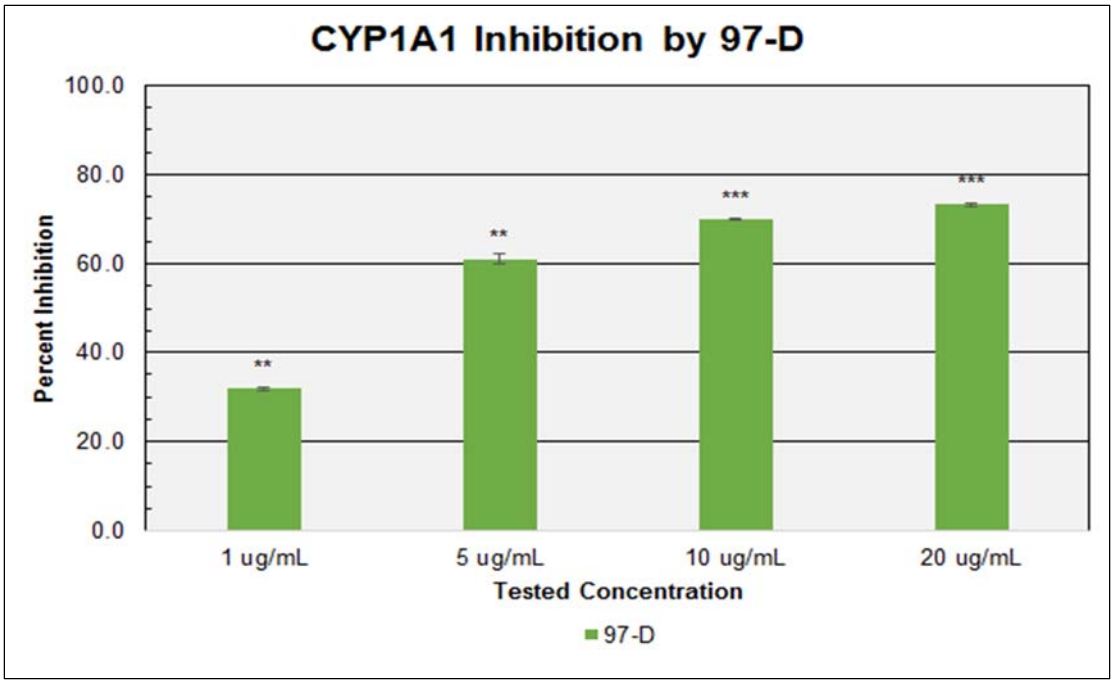

Figure 23. Effect of Incremental Concentrations of Fraction 97-D on CYP1A1.

Fraction 78-H was used to generate the 97-series fractions, so the entire 78-series was screened at a concentration of 10 µg/mL. This dosage was decreased from assays screened with the 97-series, as this was effort to preserve the bioassay – guided fractionation strategy. A graph displaying this data can be seen below in Figure 24. When tested at this concentration it was shown that 78-A showed an inhibition value of 74.7%, 78-B showed 58.2%, 78-C showed 66.0%, 78-D showed 73.3%, 78-E showed 71.1%, 78-F showed 29.1%, 78-G showed 55.2%, 78-H showed 60.8%, and 78-Q showed 40.7%.

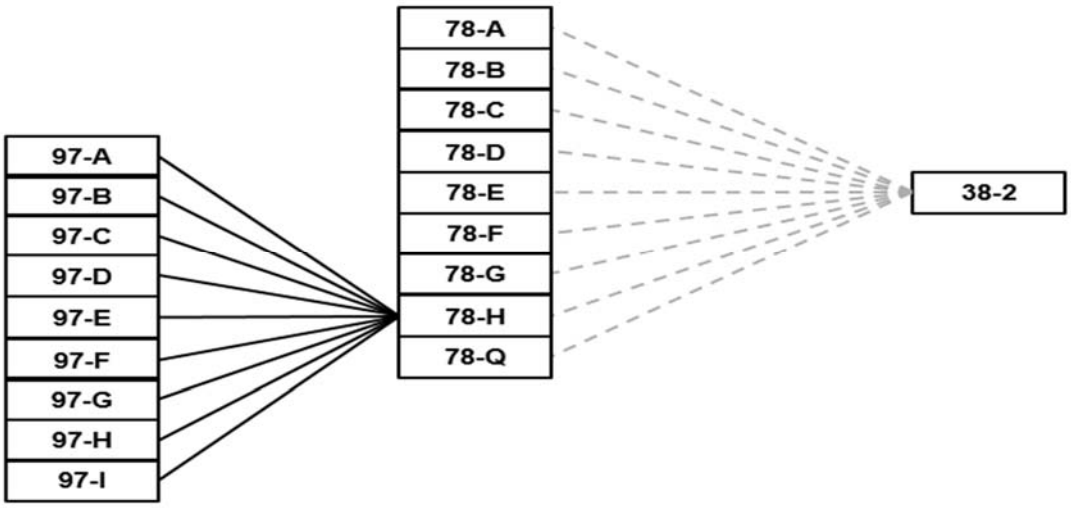

Scheme 6. Backtracking the 97-series Fractions to Parent Fraction 78-H.

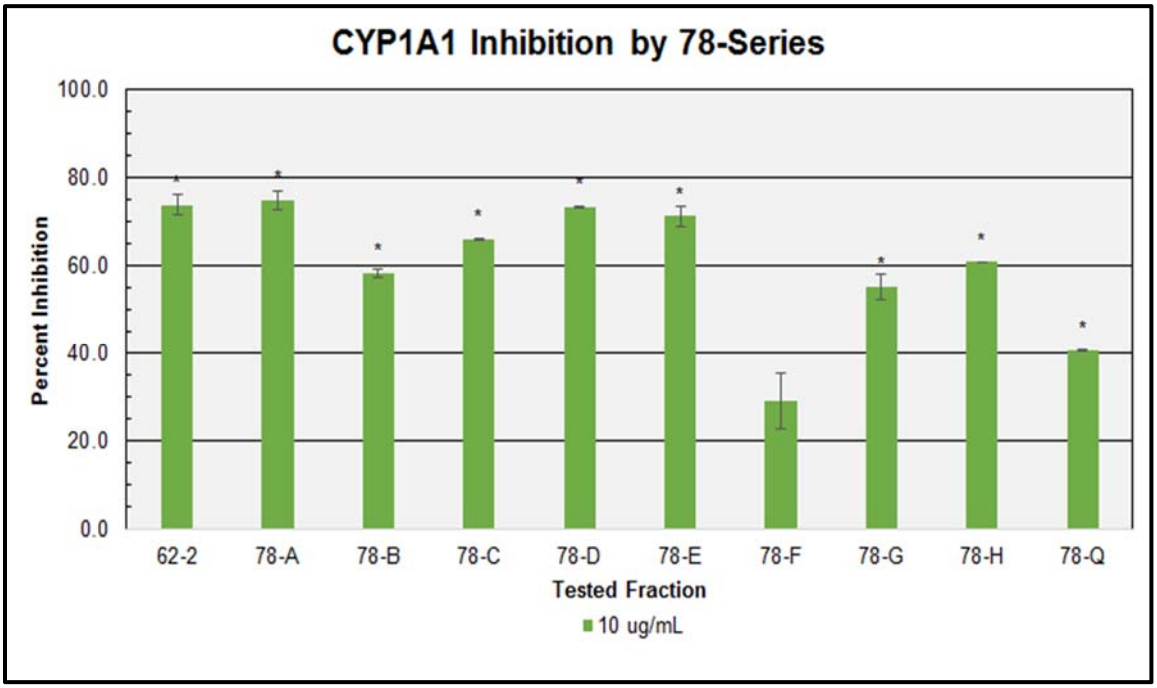

Figure 24. Screening of the 78-series Fractions on CYP1A1.

The 62-series had been previously screened at a concentration of 20 µg/mL as mentioned in section 3.2.2 above, which proved to have little effect on CYP1A1. A graph containing this data can be seen below in Figure 25. Inhibition values observed from screening the 62-series fractions at 20 µg/mL were 11.7% for 62-1, 38.1% for 62-2, 74.7% for 62-3, 69.2% for 62-4, and 62.7% for 62-5. Fraction 62-2 was the parent fraction of the 78-series and showed a low inhibition value of 38.1% when tested at 20 µg/mL. Compared to the parent fraction 38-2, which was screened alongside the 62-series fractions and gave an inhibition value of 67.8%, only fractions 62-3 and 62-4 demonstrated more potent inhibition. These fractions were not further investigated, and the reasoning for this is explained in the later section 3.2.5. Although fairly prominent inhibition was observed throughout the 97-series, it was tested at such a high concentration that it is not physiologically relevant. It is also known that the CYP450 family will catalyze a wide breadth of substrates and that screening at such a high concentration of a pure compound can induce competitive inhibition naturally.

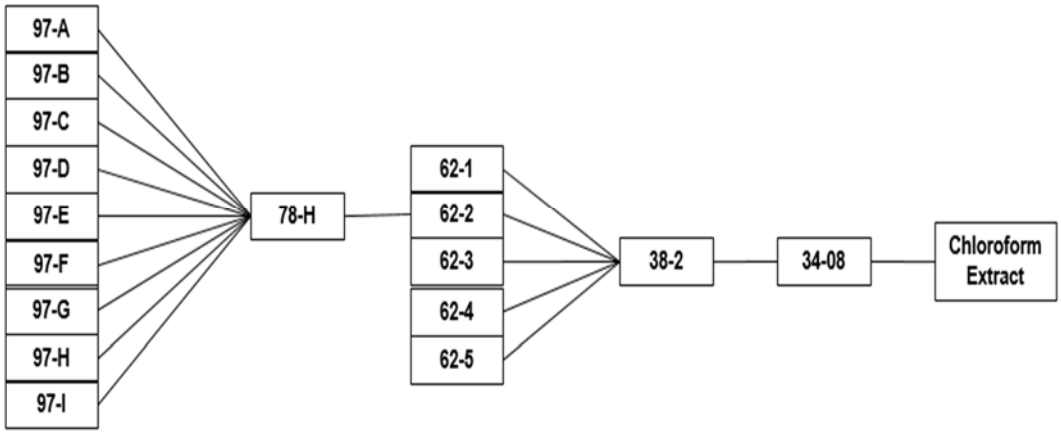

Scheme 7. Backtracking the 78-series Fractions to Parent Fraction 62-2.

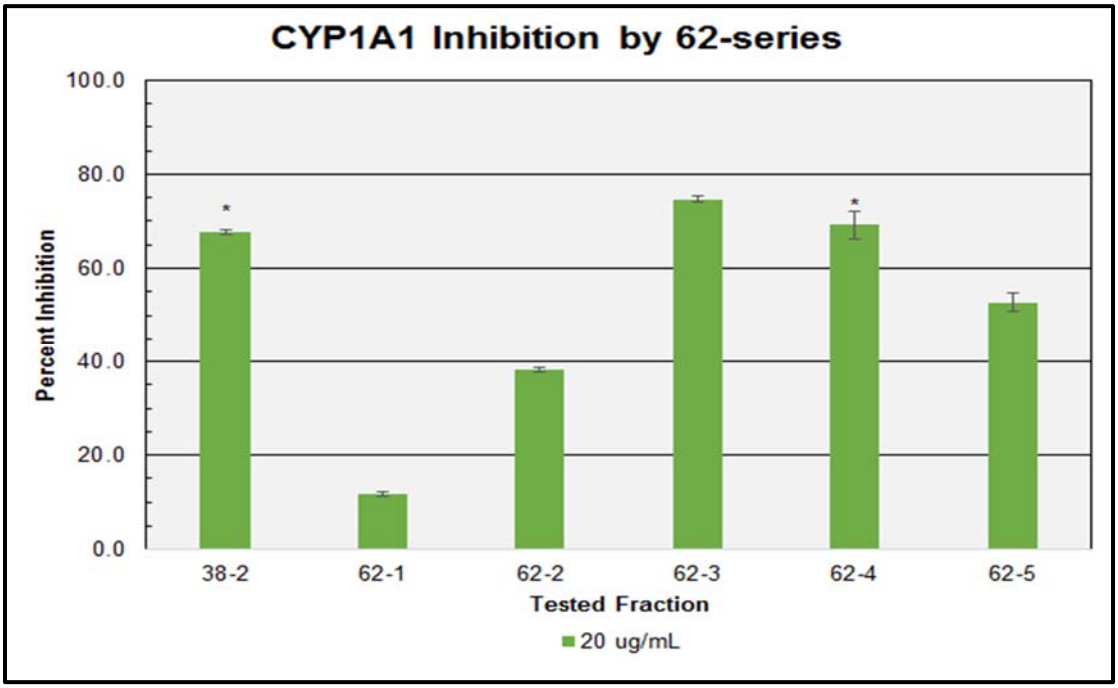

Figure 25. Screening of the 62-series Fractions on CYP1A1.

3.2.5 The 86-Series Compounds

Due to the fraction 38-6/7/8 being unavailable at the time the rest of the 38-series was screened, it was of interest to screen that fraction along with its subsequent fractionations the 86-series. Because fraction 38-6/7/8 was not tested prior to the 86-series screening, it was unknown whether this series would have any inhibitory effect. It had been observed in prior assays using more purified compounds that a concentration of 20 µg/mL was much too high, so in effort to negate the chances of observing false inhibition the dosage was dropped to 10 µg/mL. Below in Figure 26 a graph containing data from the 86-series assay is shown. When tested at this dosage fraction 38-6/7/8 displayed an inhibition value of 73.2%, 86-1 displayed 0.00%, 86-2 displayed 32.8%, 86-3 displayed 72.2%, 86-4 displayed 62.5%, 86-5 displayed 75.0%, 86-6 displayed 49.2%, and 86-7 displayed 0.00%. Despite dropping the inhibitor concentrations down, it was still difficult to determine which fractions truly had the greatest inhibitory effect. It was decided that the 38-series fractions would be tested at much lower doses, in an attempt to differentiate potent inhibition.

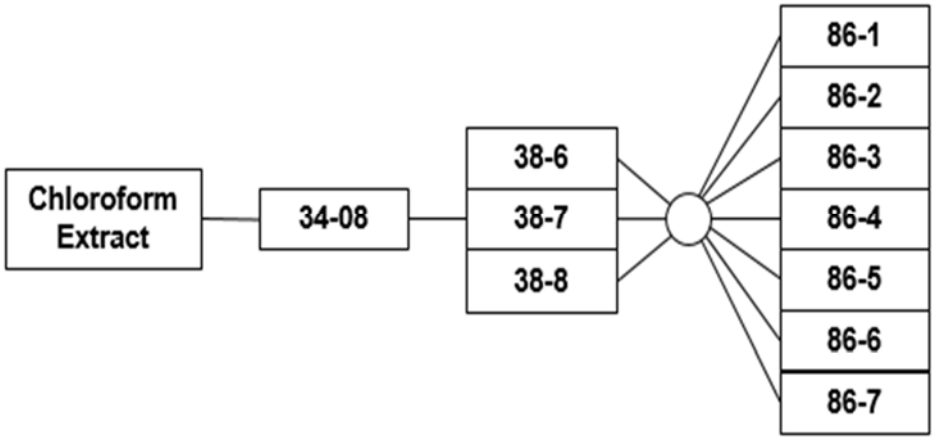

Scheme 8. Generation of the 86-series Fractions from Parent Fraction 38-6/7/8.

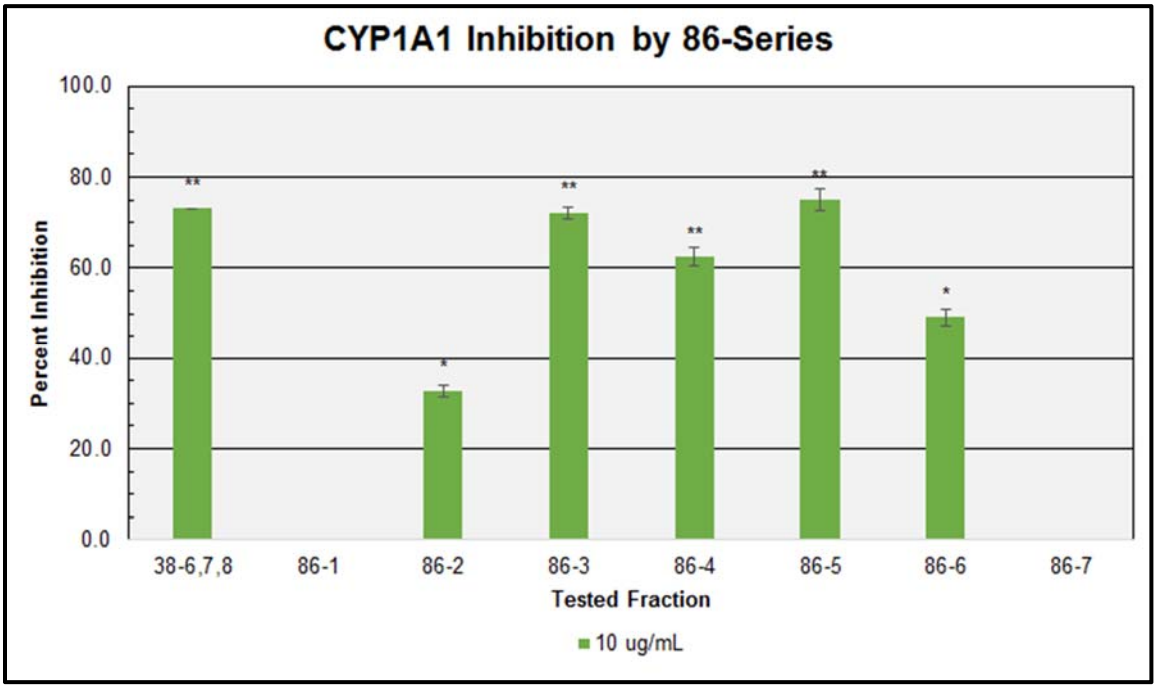

Figure 26. Screening of the 86-series Fractions on CYP1A1.

3.2.6 Revisiting 38-Series Compounds and Subsequent Fractions

In an effort to identify the chief constituent contained within the crude chloroform extract responsible for the potent CYP1A1 enzyme inhibition, the 38-series fractions were screened at a concentration of 0.5 µg/mL and 1.0 µg/mL. Figure 27 shown below, compares data collected from assaying the 38-series fractions at concentrations of 0.5 µg/mL, 1.0 µg/mL, and 20 µg/mL. The observed trend that most fractions displayed apparent inhibition when tested at higher concentrations first arose when testing the 38-series fractions. Recalling from the data collected from the 34-series fraction screening at 20 µg/mL, fraction 34-8 was by far the greatest inhibitor and was separated into the 38-series fractions. Results gathered from screening the 38-series at 20 µg/mL showed that fractions 38-4 and 38-5 had little effect on the 1A1 enzyme, and were not included in the screening at lower concentrations. Also since screening fraction 38-6/7/8 and its subsequent 86-series fractions generated questionable results, fraction 38-6/7/8 was included in the assay.

Upon screening at a concentration of 1.0 µg/mL, it was observed that fraction 38-1 showed an inhibition value of 47.4%, fraction 38-2 showed 16.1%, fraction 38-3 showed 46.2%, and the pooled fraction 38-6/7/8 showed 25.7%. When compared to the parent fraction 34-8, which displayed an inhibition value of 33.5%, only fractions 38-1 and 38-3 showed a noticeably increased effect. However, results gathered from fraction 38-3 have a standard deviation of ±3.11 AU and a calculated p – value of 0.0098, while results from 38-1 show a standard

deviation of ±8.10 AU and a calculated p – value of >0.05. When the dosage was dropped to half of what was described previously, 0.5 µg/mL, an inhibition value of 14.1% was observed for fraction 38-1, 22.2% for fraction 38-2, 31.8% for 38-3, and 23.1% for 38-6/7/8. The parent fraction 34-8 showed a value of 25.1%, which was only outperformed by fraction 38-3. Data collected from screening with 38-3 showed a standard deviation of ±1.16 AU and a calculated p – value <0.05. It was determined at this point to proceed with screenings of the 61-series and 63-series fractions using the lowered concentrations as mentioned within this section.

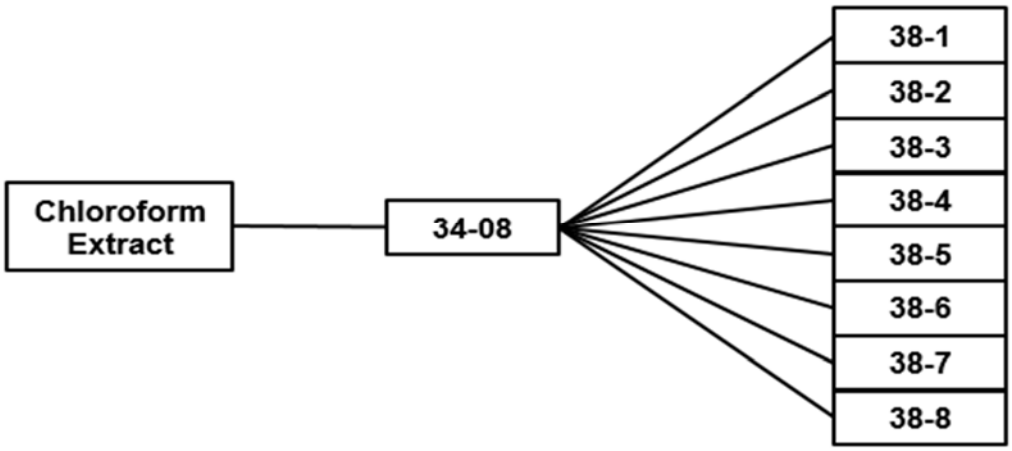

Scheme 9. Generation of the 38-series Fractions from Parent Fraction 34-08.

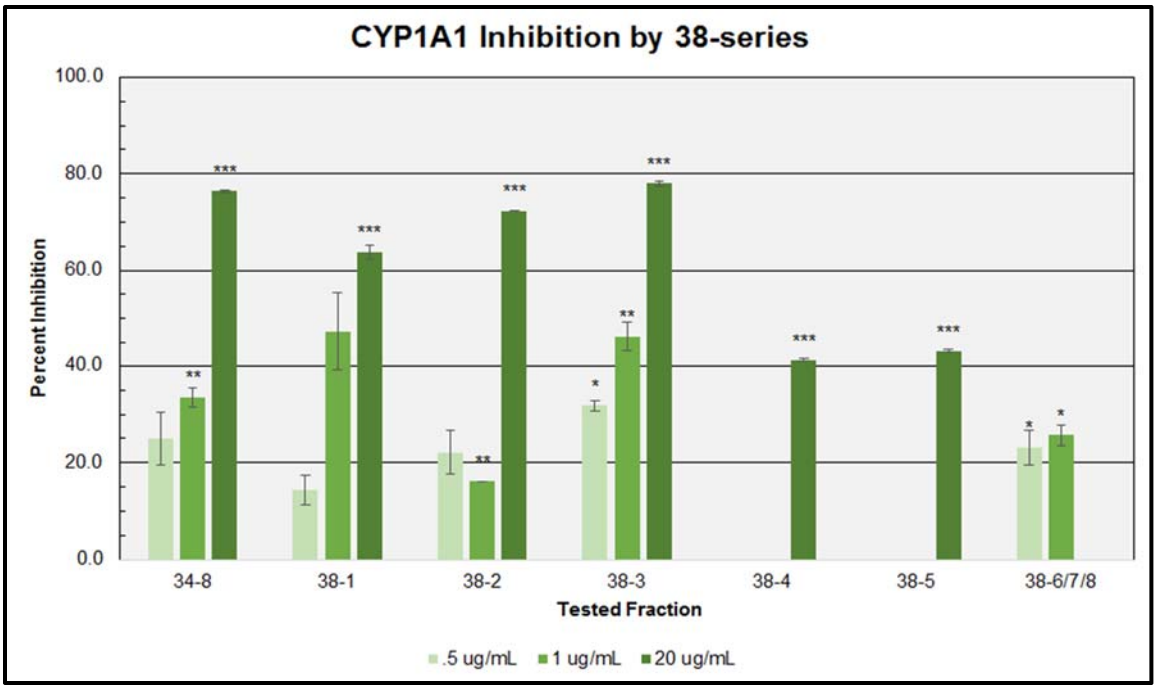

Figure 27. Screening of the 38-series Fractions at Lower Concentrations on CYP1A1.

Although data collected from samples containing fraction 38-1 showed poor inhibition when tested at a concentration of 0.5 µg/mL, it was the only other sample that showed comparable inhibition to fraction 38-3 at a concentration of 1.0 µg/mL, despite the questionable statistics. Also, subsequent fractionations of 38-2 had been tested as a separate piece of this project, which showed relatively low inhibition for the concentration at which they had been tested at; further experiments regarding the 86-series, separated from the fraction 38-6/7/8, were not pursued as data collected from the 38-series screenings showed a stagnated inhibition value around 25%.

A graph comparing the data collected from 61-series screening at 0.5, 1.0, and 20 µg/mL can be found below in Figure 28. When assays were performed to screen the 61-series fractions in the presence of 1.0 µg/mL of the fractionated extract, observed inhibition for fraction 61-1 was 4.47%, fraction 61-2 was 4.27%, fraction 61-3 was 14.1%, fraction 61-4 was 28.4%, 61-5 was 19.7%, fraction 61-6 was 25.4%, and the chromatograms generated from 61-7 assays were uninterpretable. At a tested concentration of 0.5 µg/mL, fraction 61-1 showed an inhibition value of 1.07%, 61-2 showed 3.39%, 61-3 showed 0.36%, 61-4 showed 12.4%, 61-5 showed 14.1%, 61-6 showed 8.73%, and 61-7 showed 6.47%. It was also shown that data collected during the screening of 38-1 mentioned earlier, was indeed an artifact, as the parent fraction 38-1 showed an inhibition value of 5.95% at 0.5 µg/mL and only 11.9% at 1.0 µg/mL. Due to the rather poor inhibition observed from screening the 61-series, further investigated was not pursued.

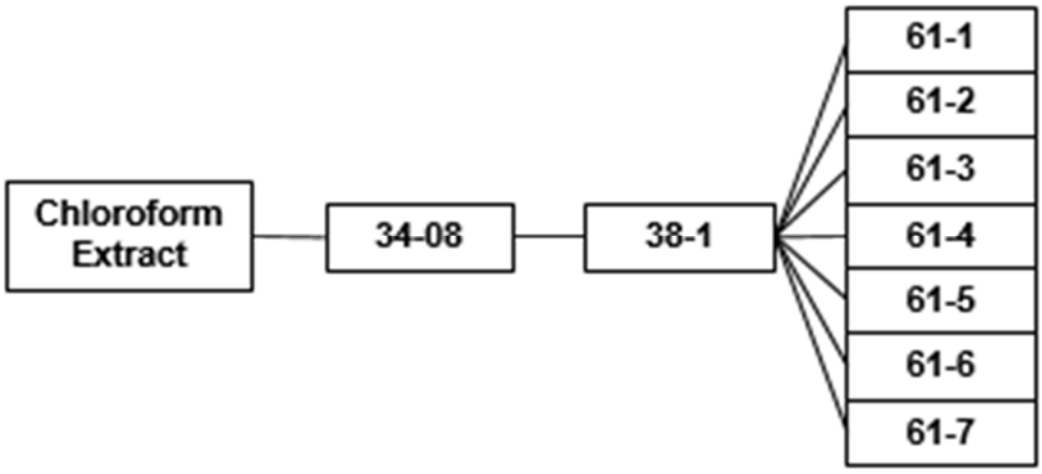

Scheme 10. Generation of the 61-series Fractions from Parent Fraction 38-1.

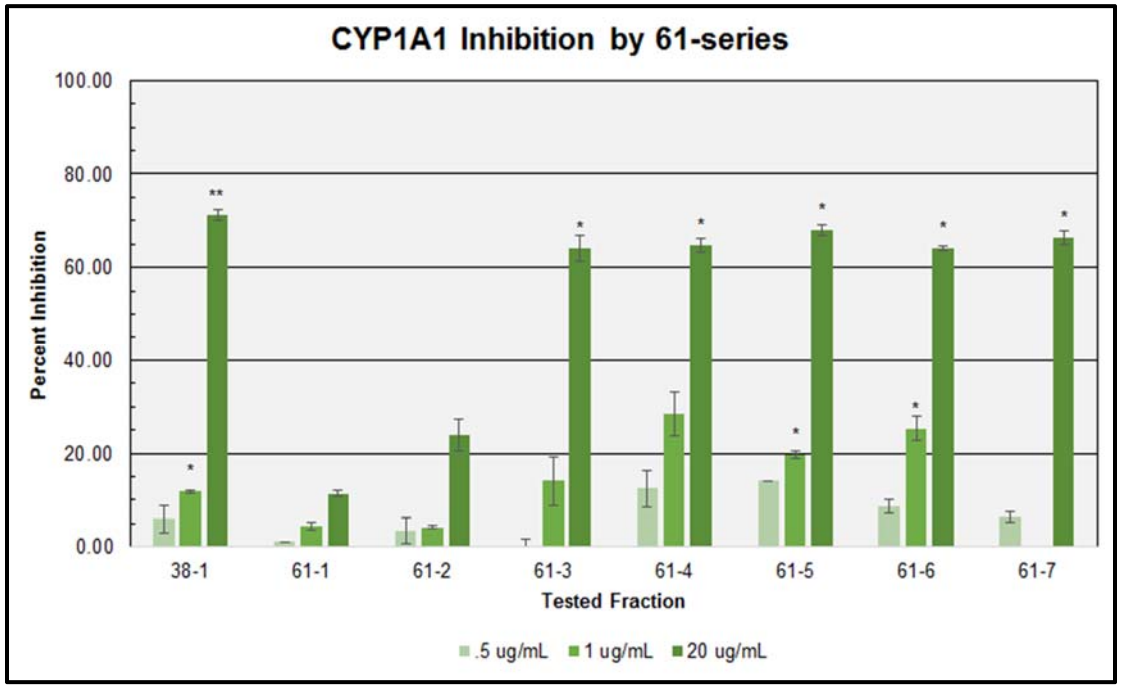

Figure 28. Screening of the 61-series Fractions on CYP1A1.

As indicated by data gathered from the 38-series screenings at low concentrations, fraction 38-3 appeared to contain a constituent that was majorly responsible for the inhibition observed in the chloroform extract, although not entirely. Initially, prior to the deviation of the activity guided fractionation scheme, the 63-series fractions had been tested at concentrations of 20, 10, and 5 μg/mL. Data collected from these experiments showed the majority of the tested fractions displayed inhibition values greater than 50%, however, the parent compound 38-3 showed the greatest inhibitory effect of all testes fractions. These assays had not included fraction 63-4 in the experiments due to unavailability at the time. Upon the screening of the 63-series at low concentrations, fraction 63-4 had been reacquired and was used in the experiments. Data gathered pertaining to experiments gathered at tested concentrations of 20, 10, 5.0, 1.0, and 0.5 μg/mL of the 63-series fractions can be seen below in Figure 29. At a concentration of 1 μg/mL, fraction 63-1 showed an inhibition value of 5.41%, 63-2 showed 19.3%, 63-3 showed 22.3%, 63-4 showed 36.9%, 63-5 showed 10.2%, and 63-6 showed 3.74%. Upon comparison of the parent fraction 38-3, which displayed an inhibitory effect of 27.1%, only results collected from fraction 63-4 gave a larger inhibition value, and had a standard deviation of ±1.12 and a calculated p – value of <0.01. To confirm the claim that fraction 63-4 was a potent inhibitor, the concentration present was dropped to 0.5 μg/mL. When tested at this dosage, fraction 63-1 resulted in an inhibition value of 3.90%, 63-2 resulted in a value of 6.13%, 63-3 resulted in a

value of 10.3%, 63-4 resulted in a value of 21.7%, 63-5 resulted in a value of 12.8%, and 63-6 resulted in a value of 12.9%. Once again fraction 63-4, which showed a standard deviation of ±1.90 and a calculated p-value of <0.05, was the only fraction to exert a more potent effect than the parent fraction 38-3, which showed a value of 14.5%.

Scheme 11. Generation of the 63-series Fractions from Parent Fraction 38-3.

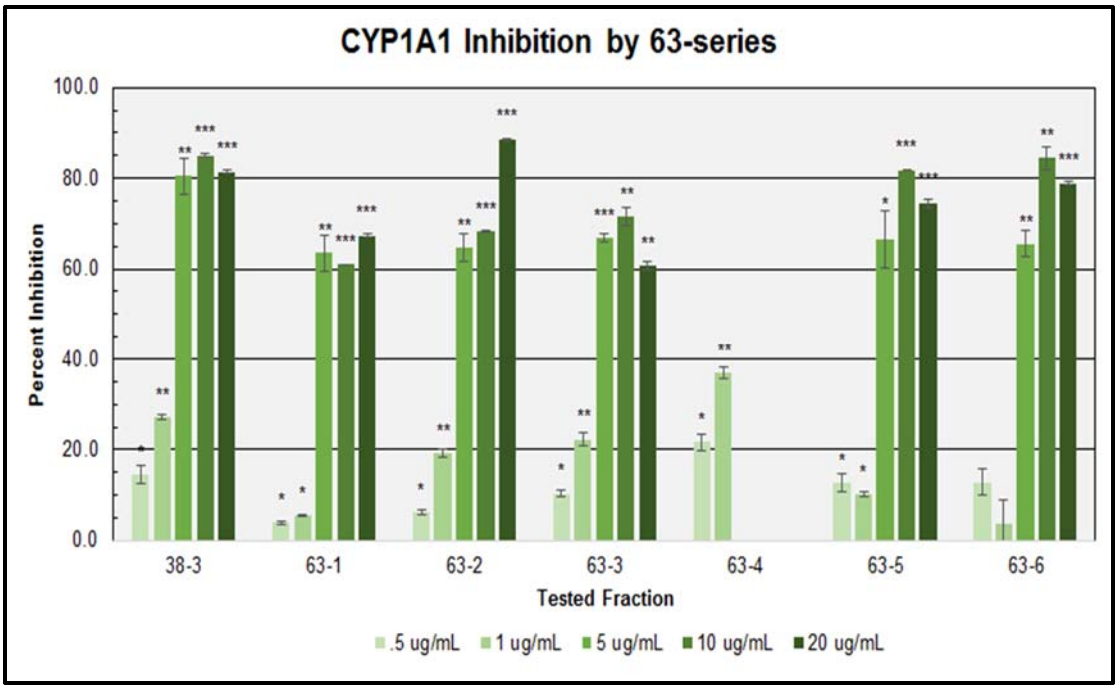

Figure 29. Screening of the 63-series Fractions on CYP1A1.

3.2.7 The 94-Series Compounds

Fraction 63-4 was separated into the 94-series fractions, whose individual fractions were relatively pure samples. Observation of fractions exerting a highly inhibitory effect would warrant purification of the fraction, and elucidation of its chemical structure. Data collected from screening the 94-series fractions can be found below in Figure 30. This series was also tested at the lowered concentrations of 1.0 µg/mL and 0.5 µg/mL, as it had been observed that there are many constituents within the açai berry extract that inhibit CYP1A1 at increased concentrations. Assays using a dosage of 1.0 µg/mL resulted in 22.7% inhibition for 94-A, in 20.4% inhibition for 94-B, in inhibition 73.4% for 94-C, in 57.1% inhibition for 94-E, in 27.2% inhibition for 94-F, in 45.6% inhibition for

94-G, in 19.8% inhibition for 94-H, and in 22.1% inhibition for 94-I. Upon comparison to the parent fraction 63-4, which gave an inhibition value of 40.6% in the presence of 1.0 µg/mL, fractions 94-C, 94-D, and 94-G showed an increased inhibitory effect. When tested at a concentration of 0.5 µg/mL, results were shown to be 18.7% for 94-A, 4.12% for 94-B, 41.9% for 94-C, 32.7% for 94-D, 7.57% for 94-E, 6.92% for 94-F, 25.8% for 94-G, 9.12% for 94-H, and 8.59% for 94-I. At this concentration the parent fraction resulted in an inhibition value of 18.7%, which was again surpassed by fractions 94-C, 94-D, and 94-G. By far, fractions 94-C and D displayed the most potent inhibition, but the inhibition observed from testing 94-D is believed to be caused by the same constituent found in fraction 94-C. This is a common effect resulting from the process of preparative liquid chromatography. results gathered from enzyme reactions in the presence of 1.0 µg/mL fraction 94-C gave a standard deviation of ± 0.018% and a calculated p-value of < 0.001, while data collected at the lowered dosage of 0.5 µg/mL showed a resulting standard deviation of ± 0.79% and a calculated p-value of < 0.05. Data collected from screening fraction 94-G at 1.0 µg/mL displayed a standard deviation of ± 0.23% and a calculated p-value of < 0.001, and at a dosage of 0.5 µg/mL showed a standard deviation of ± 5.99% and a calculated p-value of > 0.05. Due to the lesser potency of fraction 94-G, as well as the less significant data collected at 0.5 µg/mL, it was decided to pursue structure elucidation with fraction 94-C.

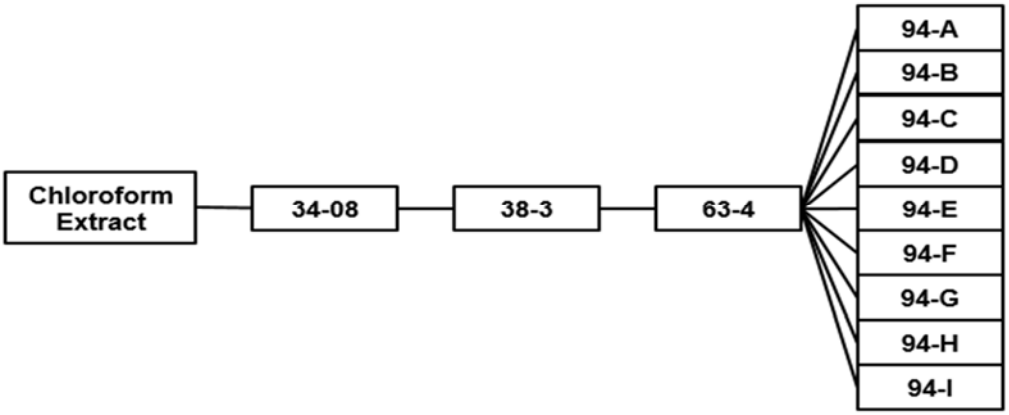

Scheme 12. Generation of the 94-series Fractions from Parent Fraction 63-4.

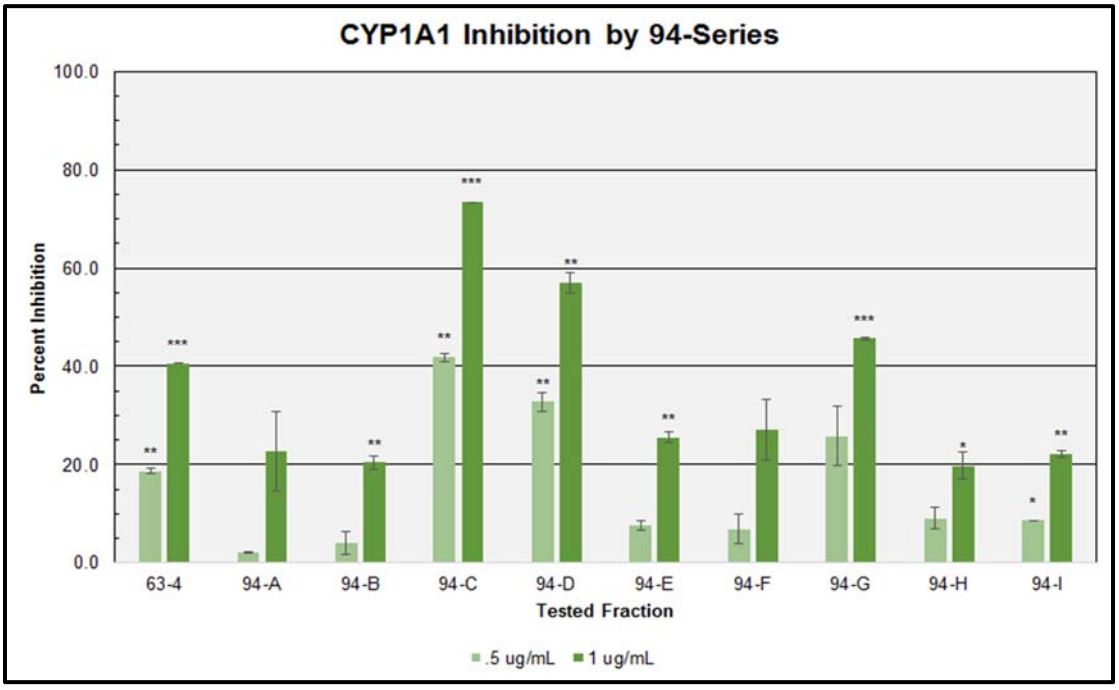

Figure 30. Screening of the 94-series Fractions on CYP1A1.

3.3.0 Structure Elucidation of Fraction 94-C

Structure elucidation of fraction 94-C was carried out by the Oberlies' laboratory, the collaborating group in this project. Using a variety of nuclear magnetic resonance applications, in particular ^{1}H-NMR, ^{13}C-NMR, COSY, HSQC, and HMBC, data were collected to determine the structure of the constituent found in fraction 94-C, which is listed in Figure 31. The molecule responsible for the potent inhibition of CYP1A1 was found to be 5,7,3'-trihydroxy-4'-methoxyflavone, which is more commonly referred to as diosmetin. Diosmetin belongs to the large family termed the polyphenols, but is more specifically identified as a flavone. The structure of diosmetin can be seen above the generated NMR data.

Diosmetin

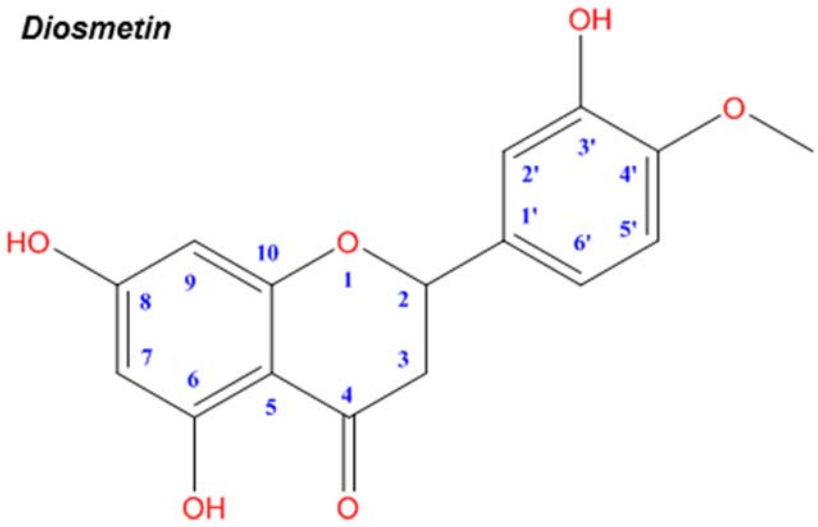

Position	δC	δH, m	COSY	HMBC
2	163.7			
3	103.3	6.92, *s*		2, 4, 10, 1'
4	181.9			
5	161.5			
6	98.9	6.19, *d*		5, 7, 8, 10
7	164.2			
8	94.1	6.51, *d*		6, 7, 9, 10
9	157.4			
10	103.7			
1'	121.5			
2'	110.2	7.56, *s*		3', 4', 6'
3'	150.7			
4'	148.0			
5'	115.7	6.93, *dd*	6'	1', 4'
6'	120.4	7.56, *dd*	5'	2, 2', 3'
5-OH		12.98, *s*		5, 6, 10
7-OH				
3'-OH				
4'-OH	56.0	3.89, *s*		4'

Figure 31. NMR Data Pertaining to the Structure of Fraction 94-C. Data was collected by collaborators from the Oberlies' group, and was found to be 5,7,3'-trihydroxy-4'-methoxyflavone (shown above chart as "diosmetin").

3.3.1 Comparison of Fraction 94-C and Diosmetin

In order to show that diosmetin was indeed the molecule found in fraction 94-C that was responsible for CYP1A1 inhibition, crystalline diosmetin was purchased to compare its effect to fraction 94-C. A substrate dependent assay was used to generate a Michaelis – Menten plot, which could then be interpreted to find a K_i value. Comparison of these K_i values generated by the purchased diosmetin and fraction 94-C, should bear similar results, which would confirm the statement that diosmetin is a very potent inhibitor of CYP1A1.

An experiment was performed varying substrate concentrations from 0.0 µM to 250 µM in the presence of 0.0 µg/mL fraction 94-C, 0.5 µg/mL fraction 94-C, and 1.0 µg/mL 94-C. A Michealis – Menten plot from this experiment can be found in Figure 32. Results show a K_m of 21.7 ± 7.00 µM and a V_{Max} of 1110 AU for the controlled reaction. In the presence of 1.0 µg/mL fraction 94-C an apparent K_m of 74.6 ± 9.29 µM and V_{Max} of 2470 AU were determined, while in the presence of 0.5 ng/mL fraction 94-C a K_m of 102.5 ± 23.1 µM and V_{Max} of 1000 AU were determined. Because a decreasing effect was not observed on the V_{Max}, this variable was set to a constant 1250 AU for each data set. It was found that in the presence of 1.0 µg/mL fraction 94-C the K_i was 0.42 ± 0.09 µg/mL, and at the lower 0.5 µg/mL dosage the K_i was 0.13 ± 0.04 µg/mL.

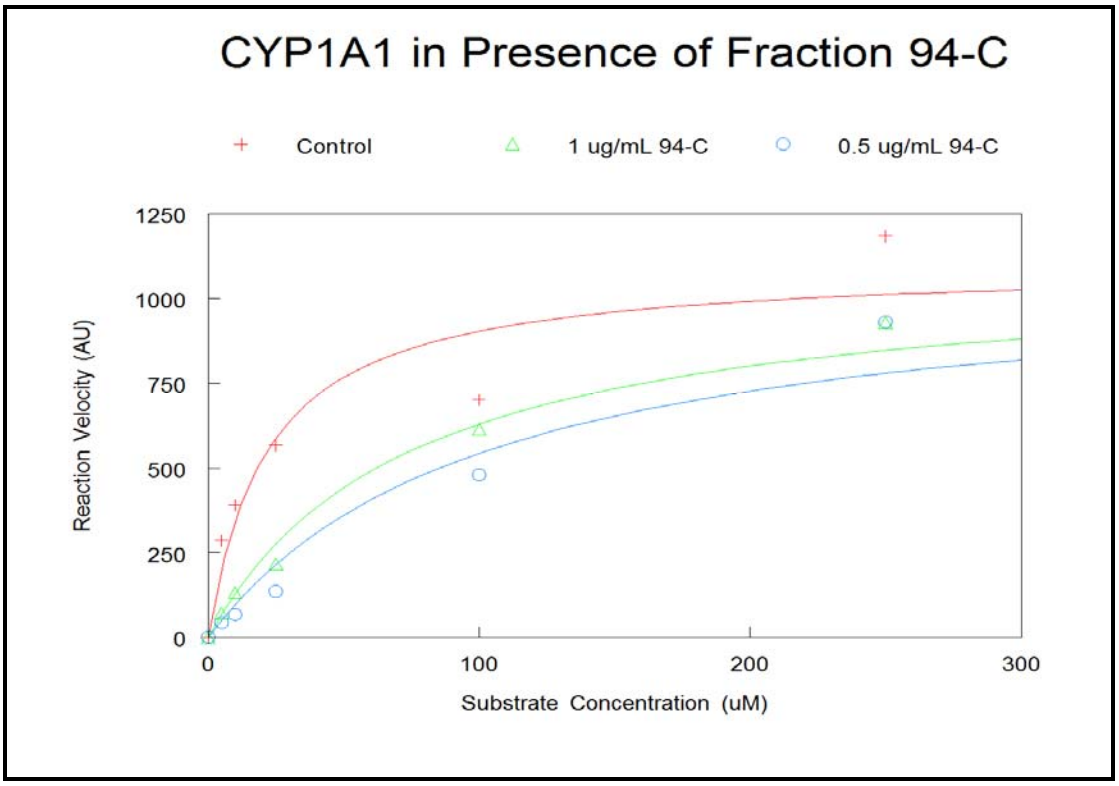

Figure 32. Michealis – Menten Plot of CYP1A1 in the Presence of Fraction 94-C.

A similar assay was performed with the CYP1A1 isoform using a purchased diosmetin standard, rather than the fractionated sample 94-C. Results from this experiment can be found in Figure 33. Substrate concentrations were varied from 0.0 to 250.0 μM in the presence of 0.0 ng/mL diosmetin, 100 ng/mL diosmetin, and 500 ng/mL diosmetin. From the controlled samples a K_m of 42.4 ± 19.9 μM and a V_{max} of 1291.0 AU were determined. While in the presence of 500 ng/mL diosmetin a K_m of 93.8 ± 46.5 μM and a V_{max} of 1139.9 AU were determined, while in the presence of 100 ng/mL diosmetin a K_m of 82.2 ± 48.0 μM and a V_{max} of 1244.2 AU were determined. Using this information a K_i for the 500 ng/mL reactions was found to be 412 ± 199 ng/mL,

and in the 100 ng/mL reactions a K_i of 106 ± 55.8 ng/mL was calculated. Results gathered from the use of the purchased diosmetin standard show similar calculated K_i values compared to the data gathered with fraction 94-C. However, this was expected as the fraction 94-C was relatively pure, and these results confirm that diosmetin is the constituent responsible for inhibition.

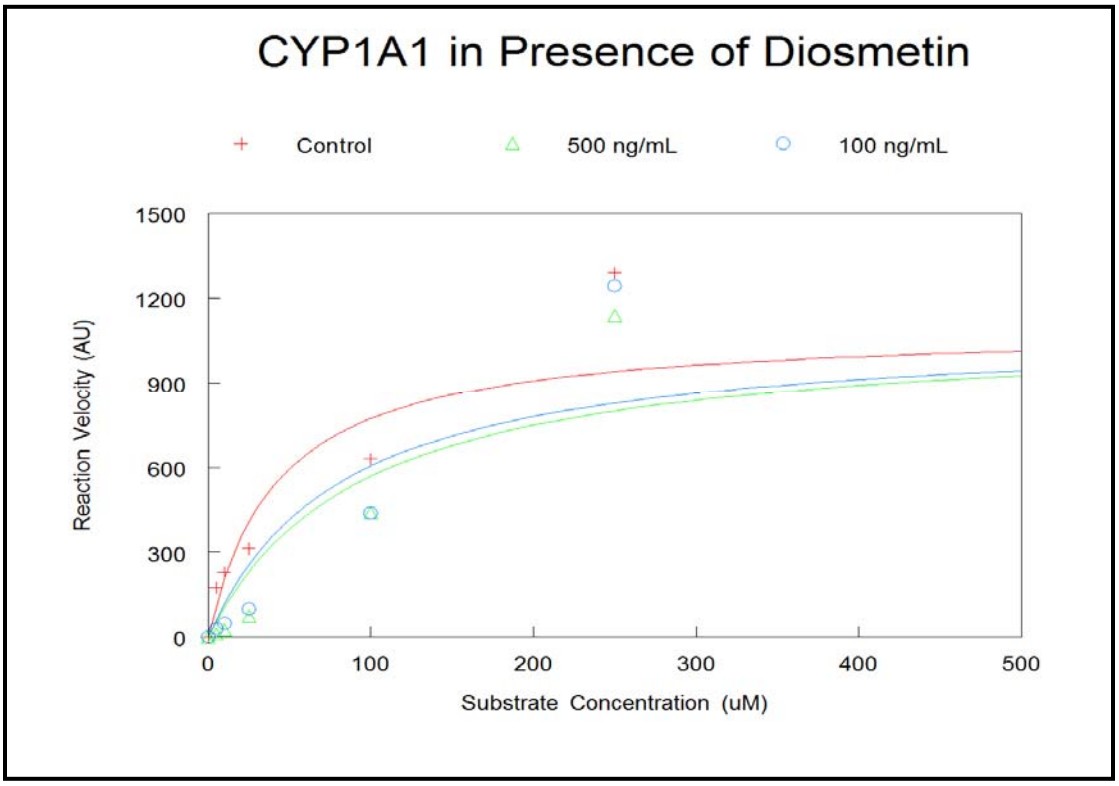

Figure 33. Michealis – Menten Plot of CYP1A1 Activity in the Presence of Purchased Diosmetin.

CHAPTER IV

CONCLUSION

In the presence of the initial, four, crude extracts of acai berry, CYP1A2 showed no apparent inhibition, even at very high dosages. It is important to investigate possible interactions with the CYP1A2 isoform, as the number of its pharmaceutical substrates has increased largely over the past decade. Results are indicative that concomitant intake of a pharmaceutical metabolized by CYP1A2 and açai berry should have no potential pharmacokinetic interactions and may be deemed as safe.

It was also shown that the Chloroform extract had an extremely potent inhibitory effect on CYP1A1 enzyme reactions. Initial screening of the crude chloroform extract with CYP1A1 showed a remarkable 79.2% inhibition, when tested at the lowest dosage of 10 μg/mL. The chloroform extract was subjected to several rounds of inhibition-directed based fractionations. Shown below in scheme 12 is a detailed summary of the results from screening açai berry extracts, which shows the inhibitory effect observed on CYP1A1 O-deethylation of 7-ethoxycoumarin.

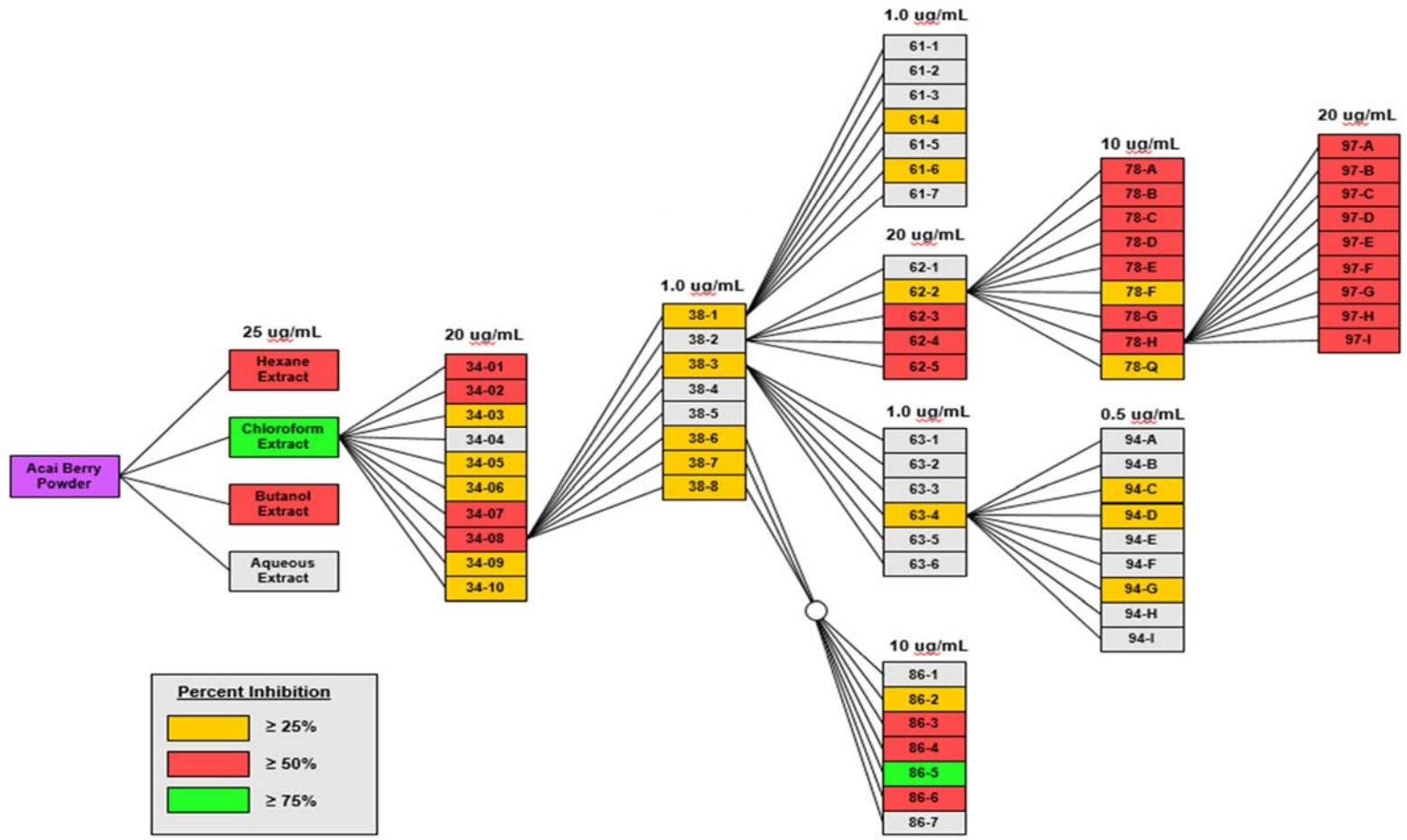

Scheme 13. Bioassay Guided Fractionation Diagram Depicting Results from CYP1A1 Isoform Screenings. Diagram shows the observed inhibition seen in CYP1A1 catalyzed 7-ethoxycoumarin deethylation reaction while in the presence of açai berry fractions.

Because fractions 38-1, 38-2, 38-3, and 38-6/7/8 displayed modest inhibition when tested at dosages ranging from 10 – 20 µg/mL, it can be said that many constituents contained within the chloroform extract are inhibitors of CYP1A1 at high concentrations. However, when tested concentrations were lowered to more physiological relevant levels (500 ng/mL and 1 µg/mL), only fraction 38-3 displayed modest inhibition. Subsequent fractionations of 38-3 revealed that fraction 94-C contained the primary constituent responsible for the observed inhibition. Structure elucidation found that 5,7,3'-trihydroxy-4'-methoxyflavone, more commonly known as diosmetin, was the major compound in fraction 94-C. Diosmetin is a methoxylated flavone, a class of flavonoid molecules that has recently shown promise in affecting cancinogenesis. Studies investigating 5,7-dimethoxyflavone's effect on CYP1A1 showed that this methoxylated flavone exerted a potent effect at 1 – 2 µM concentrations[58]. However, results found in this project show that the cruder fraction 94-C has a K_i of 0.327 µg/mL at a dosage of 1.0 µg/mL 94-C and 0.243 µg/mL at 0.5 µg/mL, while the purchased standard of diosmetin gave an observed K_i of 9.23 ng/mL at a concentration of 500 ng/mL and 2.51 ng/mL at a 100 ng/mL concentration.

A previous study conducted by Ciolino et al. in 1998, also found diosmetin to be a potent inhibitor of CYP1A1[73]. Results from this study found an IC_{50} value of 30.0 nM using DMBA – induced CYP1A1 enzymes. Although these are two different values used to evaluate enzyme inhibition, both values were found to be in the nanomolar range, which is consistent as to what was found in this study.

Inhibition of CYP1A1 enzymatic catalysis is quite important, as it is a means to decrease the bioactivation of carcinogen compounds within the body. Past works evaluating the bioavailability of diosmetin after consumption, have shown serum plasma concentrations ranging from a few ng/mL to several hundred ng/mL following the same oral dosages of 400 – 600 mg diosmetin. A more recent study using HPLC-MS/MS methodology reported that following consumption of diosmetin, its glucuronide form was detected and reached levels up to 10 ng/mL, however, concentrations of free diosmetin were below the detection limit of 50 pg/mL[74]. Further work still is required to confirm and clarify this finding.

In summary, constituents within the açai berry appear to no effect on the CYP1A2 isoform, but have a much greater effect on its close relative CYP1A1. As CYP1A1 is not largely responsible for metabolism of pharmaceutical drugs, this suggests that concomitant intake of prescribed pharmaceuticals and açai berry appears safe. Diosmetin has been shown to account for a small percentage of the total crude, açai, plant material, which would require the consumption of a considerable amount of açai berry to observe a chemopreventative effect. Screening of açai berry extracts with other CYP450 isoforms in this project has shown that only CYP2E1 was affected by diosmetin, and it appears to have some effect on cell culture modeling of the antioxidant response element pathway. Current research is also evaluating the antioxidant effect of diosmetin in cell culture studies.

REFERENCES

1) Jakoby, W. B.; Ziegler D. M. The Enzymes of Detoxification. *J. Bio. Chem.*, **1990**, *256*(34), 20715-20718.

2) Ding, X.; Kaminsky, L. S. Human Extrahepatic Cytochromes P450: Function in Xenobiotic Metabolism and Tissue-Selective Chemical Toxicity in the Respiratory and Gastrointestinal Tracts. *Annu. Rev. Pharmacol. Toxicol.*, **2003**, *43*, 149-173.

3) Anzenbacher, P.; Anzenbacherová, E. Cytochrome P450 and Metabolism of Xenobiotics. *Cell. Mol. Life Sci.*, **2001**, *58*(5), 737-747.

4) Pirmohamed, M.; Kitteringham N. R.; Park, B. K. The Role of Active Metabolites in Drug Toxicity. *Drug Saf.*, **1994**, *11*(2), 114-144.

5) Draggan, S. Excretion of Toxicants. *En. of Earth*, **2006**. http://www.eoearth.org/view/article/152706/.html (accessed Oct 15, 2015).

6) Axelrod, J. The Enzymatic Demethylation of Ephidrine. *J. of Pharmacol.*, **1955**, *114*, 430-438

7) Brodie, B.; Axelrod, J.; Cooper, R.; Gaudette, L.; LaDu, B. N.; Mitoma, C.; Udenfriend S. Detoxication of Drugs and Other Foreign Compounds by Liver Microsomes. *Science*, **1955**, *121*, 603-604.

8) Poulos, T. L.; Johnson, E. F. Structures of Cytochrome P450 Enzymes. In *Cytochrome P450*, 3rd ed.; Ortiz de Montellano, P. R., Ed.; Springer: New York, **2005**, pp 87-114.

9) Garfinkel, D. Studies on Pig Liver Microsomes. I. Enzymatic and Pigment Composition of Different Microsomal Fractions. *Archives of Biochemsitry and Biophysics*, **1958**, *77*, 493-509.

10) Klingenberg M. Pigments of Rat Liver Microsomes. *Archives of Biochemistry and Biophysics*, **1958**, *75*, 376-86.

11) Denisov, I. G.; Makris, T. M.; Sligar, S. G.; Schlichting, I. Structure and Chemistry of Cytochrome P450. *Chem. Rev.*, **2005**, *105*(6), 2253-2277.

12) Sheweita, S. A. Drug-Metabolizing Enzymes: Mechanisms and Fnctions. *Curr. Drug Metab.* **2000**, *1*(2), 107-132.

13) Meunier, B.; de Visser, S. P.; Shaik, S. Mechanism of Oxidation Reactions Catalyzed by Cytochrome P450 Enzymes. *Chem. Rev.* **2004**, *104*(9), 3947-3980.

14) Paine, M. F.; Hart, H. L.; Ludington, S. S.; Haining, R. L.; Rettie, A. E.; Zeldin, D. C., The Human Intestinal Cytochrome P450 "Pie". *Drug Metab. Dispos.*, **2006**, *34*(5), 880-886.

15) Meunier, B.; Bernadou, J. Active Iron-Oxo and Iron-Peroxo Species in Cytochromes P450 and Peroxidases; Oxo-Hydroxo Tautomerism with Water-Soluble Metalloporphyrins. In *Metal-Oxo and Metal-Peroxo Species in Catalytic Oxidations*; Meunier, B., Ed.; Springer: New York, **2000**; Vol. 97; p 20.

16) Tuck, S. F.; Graham-Lorence, S.; Peterson, J. A.; Ortiz de Montellano, P. R., Active Sites of the Cytochrome P450 (CYP101) F87W and F87A Mutants. Evidence for Significant Structural Reorganization without Alteration of Catalytic Regiospecificity. *J. Biol. Chem.,* **1993**, *268*(1), 269-275.

17) Denisov, I. G.; Sligar, S. G. Activation of Molecular Oxygen. In *Cytochrome P450*, 4th ed.; Ortiz de Montellano, P. R., Ed.; Springer: New York, **2015**; pp 69-109.

18) Ortiz de Montellano, P.R.; De Voss, J. Oxidizing Species in the Mechanism of Cytochrome P450. *Nat. Prod. Rep.*, **2002**, *19*(4), 477-493.

19) Schauss, A. G.; Wu, X.; Prior, R. L.; Ou, B.; Huang, D.; Owens, J.; Agarwal, A.; Jensen, G. S.; Hart, A. N.; Shanbrom, E. Antioxidant Capacity and Other Bioactivities of the Freeze – Dried Amazonian Palm Berry, *Euterpe oleraceae mart.* (Acai). *J. Agric. Food. Chem.*, **2006**, *54*(22), 8640-8610.

20) Del Pozo-Insfran, D.; Percival, S. S.; Talcott, S. T. Acai Polyphenolics in their Glycoside and Aglycone Forms Induce Apoptosis of HL-60 Leukemia Cells. *J. Agric. Food. Chem.*, **2006**, *54*(4), 1222-1229.

21) Felzenswalb, I.; da Costa Marques M. R.; Mazzei, J. L.; Aiub, C. A. Toxicological Evaluation of *Euterpe edulis*: A Potential Superfruit to be Considered. *Food Chem. Toxicol.*, **2013**, *58*, 536-544.

22) Poulose, S. M.; Bielinski, D. F.; Carey, A.; Schauss, A. G.; Shukitt-Hale, B. Modulation of Oxidative Stress, Inflammation, Autophagym and Expression of NrF2 in Hippocampus and Frontal Cortex of Rats Fed with Acai-Enriched Diets. *Nutr. Neurosci.* [Online early acces]. PMID: 26750735. Published Online: Jan 11, **2016**. http://www.pubmed.org (accessed Feb 19, 2016).

23) Peixoto, H.; Roxo, M.; Krstin, S.; Röhrig, T.; Richling E.; Wink, M. An Anthocyanin-Rich Extract of Acai Increases Stress Resistance and Retards Aging-Related Markers in *Caenorhabditis elegans*. *J. Agric. Food Chem.*, **2016**, *64*(6), 1283-1290.

24) Wrighton, S. A.; Maurel, P.; Schuetz, E. G.; Watkins, P. B.; Young, B.; Guzelian, P. S., Identification of the Cytochrome P450 Induced by Macrolide Antibiotics in Rat Liver as the Glucocorticoid Responsive Cytochrome P450. *Biochemistry*, **1985**, *24*(9), 2171-2178.

25) Huang, S. M.; Strong, J. M.; Zhang, L.; Reynolds, K. S.; Nallani, S.; Temple, R.; Abraham, S.; Habet, S. A.; Baweja, R. K.; Burckart, G. J.; Chung, S.; Colangelo, P.; Frucht, D.; Green, M. D.; Hepp, P.; Karnaukhova, E.; Ko, H. S.; Lee, J. I.; Marroum, P. J.; Norden, J. M.; Qiu, W.; Rahman, A.; Sobel, S.; Stifano, T.; Thummel, K.; Wei, X. X.; Yasuda, S.; Zheng, J. H.; Zhao, H.; Lesko, L. J., New Era in Drug Interaction Evaluation: US Food and Drug Administration Update on CYP Enzymes, Transporters, and the Guidance Process. *J. Clin. Pharmacol.* **2008**, *48*(6), 662-670

26) A. A. Walsh; G. D. Szklarz; E. E. Scott. Human Cytochrome P450 1A1 Structure and Utility in Understanding Drug and Xenobiotic Metabolism. *JBC* Online **2013**, *288*, 12932-12943.

27) Nakamura, H.; Ariyoshi, N.; Okada, K.; Nakasa, H.; Nakazawa, K.; Kitada, M. CYP1A1 is a Major Enzyme Responsible for the Metabolism of Granisetron in Human liver Microsomes. *Curr. Drug Metab.*, **2005**, *6*(5), 469-480.

28) Liu, J.; Sridhar, J.; Foroozesh, M. Cytochrome P450 Family 1 Inhibitors and Structure – Activity Relationships. *Molecules*, **2013**, *18*, 14470-14495.

29) Davis, M. P.; Glare, P. A.; Quigley, C.; Hardy, J. Individual CYP enzymes in Liver Disease. In *Opioids in Cancer* Pain, 2nd ed.; Davis, M. P.; Glare, P. A.; Hardy, J.; Quigley, C., Ed.; Oxford University Press: Oxford, **2009**; p 47.

30) Faber, M. S.; Jetter, A.; Fuhr, U. Assessment of CYP1A2 Activity in Clinical Practice: Why, How, and When?. *Basic & Clinical Pharmacology & Toxicology*, **2005**, *97*(3), 125-134.

31) National Institute of Health. Medline: Zolmitriptan. https://www.nlm.nih.gov/medlineplus/druginfo/meds/a601129.html (accessed Feb 24, 2016).

32) Taraschenko, O. D.; Barnes, W. D.; Herrick-Davis, K.; Yokoyama, Y.; Boyd, D. L.; Hough, L. B. Actions of Tacrine and Galanthamine on Histamine-N-methyltransferase. *Met. Find. Exp. Clin. Pharamacol.*, **2005**, *27*(3), 161-165.

33) Correia, M.; De Montellano, P. Inhibition of Cytochrome P450 Enzymes. In *Cytochrome P450*, 3rd ed.; de Montellano, P., Ed.; Springer: New York, **2005**; pp 247-280.

34) P450 Drug Interaction Table. http://medicine.iupui.edu/clinpharm/ddis/main-table.html (accessed Nov 6, 2015).

35) Dahlin, D.C.; Miwa, G. T.; Lu, A. Y.; Nelson, N.D. N-acetyl-p-benzoquinone imine: A Cytochrome P450-Mediated Oxidation Product of Acetaminophen. *Proc. Natl. Acad. Sci. USA.*, **1984**, *81*, 1327-1331.

36) Seis, H. Physiological Society Symposium: Impaired Epithelial and Smooth Muscle Cell Function in Oxidative Stress, Oxidative Stress: Oxidants and Antioxidants. *Exp. Phys.*, **1997**, *82*, 291-295.

37) Valko, M.; Rhodes, C. J.; Moncol, J.; Izakovic, M.; Mazur, M. Free Radicals, Metals and Antioxidants in Oxidative Stress-Induced Cancer. *Chem. Biol. Interact.*, **2006**, *160*, 1-40.

38) Wang, K. Molecular Mechanisms of Hepatic Apoptosis. *Cell Death and Disease*, **2014**, *5*, 996.

39) Hinson, J. A; Roberts, D. W.; James, L. P. Mechanisms of Acetaminophen-Induced Liver Necrosis. *Handb. Exp. Pharmacol.*, **2010**, *196*, 369-405.

40) Yi-Hua, J.; Heck, D. E.; Dragomir, A. C, Gardner, C. R.; Laskin, D. L.; Laskin, J. D. Acetaminophen Reactive Intermediates Target Hepatic Thioredoxin Reductase. *Chem. Res. Toxicol.*, **2014**, *27*(5), 882-894.

41) Laine, J. E.; Auriola, S.; Pasanen, M.; Juvonen, R. O. Acetaminophen Bioactivation by Human Cytochrome P450 Enzymes and Animal Microsomes. *Xenobiotica*. **2009**, *39*, 11-21.

42) Mitchell, J. R.; Jollow, D. J.; Potter, W. Z.; Gillette, J. R.; Brodie, B. B. Acetaminophen-Induced Hepatic Necrosis. IV. Protective Role of Glutathione. *J. Pharmacol. Exp. Ther.* **1973**, *187*, 211-217.

43) Reid, A. B.; Kurten, R. C.; McCullough, S. S.; Brock, R. W.; Hinson, J. A. Mechanisms of Acetaminophen – Induced Hepatotoxicity: Role of Oxidative Stress and Mitochondrial Permeability Transition in Freshly Isolated Mouse Hepatocytes. *J. Pharmacol. Exp. Ther.* **2005**, *312*, 509-516.

44) Hecht, S. S. Cigarette Smoking and Lung Cancer: Chemical Mechanisms and Approaches to Prevention. *Lancet Onco.* **2002**, *3*(8), 461-469.

45) Hecht, S. S. Tobacco Smoke Carcinogens and Lung Cancer. *J. Natl. Cancer Inst.* **1999**, *91*, 1194-1210.

46) Tindle, H. A.; Davis, R. B.; Phillips, R.S.; Eisenberg, D.M. Trends in Use of Complementary and Alternative Medicine by US Adults: 1997-2002. *Altern. Ther. Health. Med.* **2005**, *11*, 42-49.

47) Herman, R.; von Richter, O. Clinical Evidence of Herbal Drugs as Perpetrators of Pharmacokinetic Drug Interactions. *Plant Med.* **2012**, *78* (13), 1458-1477.

48) Kaufman D. W., Kelly J.P., Rosenberg L., Anderson T.E., Mitchell A., Recent Patterns of Medication Use in the Ambulatory Adult Population of the United States: the Slone survey. *JAMA* **2002**, *287*, 337-344.

49) Guo, L. Q.; Yamazoe, Y.; Inhibition of Cytochrome P450 by Furanocoumarins in Grapefruit Juice and Herbal Medicines. *Acta. Pharmacol. Sin.*, **2004**, *25*, 29–36.

50) Kakar, S. M.; Paine, M. F.; Stewart, P. W.; Watkins, P. B. 6'7'-Dihydroxybergamottin Contributes to the Grapefruit Juice Effect. *Clin. Pharmacol. Ther*. **2004**, *75*(6), 569-579.

51) Roth, B. D. The Discovery and Development of Atorvastatin, a Potent Novel Hypolipidemic Agent. *Prog. Me. Chem.*, **2002**, *40*(1), 1-22.

52) Lipitor Becomes World's Top – Selling Drug. http://www.crains newyork.com/article/20111228/HEALTH_CARE/111229902.html (accessed Jan 15, 2016).

53) Kopp, P. Resveratrol, a Phytoestrogen Found in Red Wine. A Possible Explanation for the Conundrum of the 'French Paradox'?. *Eur. J. Endocrinol.*, **1998**, *138*, 619-620.

54) Jang, M.; Cai, L.; Udeani, G. O.; Slowing, K. V.; Thomas, C. F.; Beecher, C. W.; Fong, H. H.; Farnsworth, N. R.; Kinghorn, A. D.; Mehta, R. G.; Cancer Chemopreventive Activity of Resveratrol, a Natural Product Derived from Grapes. *Science*, **1999**, *275*, 218-220.

55) Pervaiz, S. Resveratrol: from Grapevines to Mammalian Biology. *FASEB. J.*, **2003**, *17*, 1975–1985.

56) Middleton E. J.; Kandaswami C.; Theoharides, T. C. The Effects of Plant Flavonoids on Mammalian Cells: Implications for Inflammation, Heart Disease, and Cancer. *Pharmacol. Rev.*, **2000**, *52*, 673–751.

57) Yang, C. S.; Prabhu, S.; Landau, J. Prevention of Carcinogenesis by Tea Polyphenols. *Drug Metab. Rev.*, **2001,** *33*, 237–253.

58) Walle T. Methoxylated Flavones, a Superior Cancer Chemopreventative Flavonoid Subclass?. *Sem. Cancer*, **2007**, *17*(5), 354-362

59) Ciolino H. P.; Daschner, P. J.; Wang,t. T. T. Y.; Yeh, G. C. Effect of Curcumin on the Aryl Hydrocarbon Receptor and Cytochrome P450 1A1 in MCF-7 Human Breast Carcinoma Cells. *Biochem. Pharmacol.*, **1998,** *56*, 197–206.

60) Ciolino H. P.; Daschner, P. J.; Yeh, G. H. Dietary Flavonols Quercetin and Kaempferol are Ligands of the Aryl Hydrocarbon Receptor that Affect CYP1A1 Transcription Differentially. *J. Biochem.*, **1999**, *340* 715–722.

61) Ciolino, H. P.; Yeh, G. C. Inhibition of Aryl Hydrocarbon-Induced Cytochrome P450 1A1 Enzyme Activity and CYP1A1 Expression by Resveratrol. **1999**, *Mol. Pharmacol.*, *56*, 760–767.

62) Walle, T.; Otake Y.; Brubaker, J. A.; Walle, U. K.; Halushka, P. V. Disposition and Metabolism of the Flavonoid Chrysin in Normal Volunteers. *Br. J. Clin. Pharmacol.*, **2001**, *51*, 143–146.

63) Goldberg, D. M.; Yan, J.; Soleas G. J. Absorption of Three Wine-Related Polyphenols in Three Different Matrices by Healthy Subjects. **2003**, *Clin. Biochem*., 36, 79–87.

64) Wen X.; Walle, U. K.; Walle T. 5,7-Dimethoxyflavone Down-Regulates CYP1A1 Expression and Benzo[a]pyrene-Induced DNA Binding in Hep G2 Cells. **2005**, *Carcinogenesis*, *26*, 803–809.

65) Udani, J. K.; Singh, B. B.; Singh, V. J.; Barrett, M. L. Effects of Açai (*Euterpe oleracea Mart*.) Berry Preparation on Metabolic Parameters in a Healthy Overweight Population: A Pilot Study. *J. Nutr*., **2011**, 10-45.

66) Soares de Moura R.; Ferreira, T. S.; Lopes, A. A.; Pires, K. M. P.; Nesi, R. T.; Resende, A. C.; Souza, P. J. C.; Ribeiro da Silva, A. J.; Borges, R. M.; Porto, L. C.; Valenca S. S.; Effects of Euterpe oleracea Mart. (AÇAÍ) Extract in Acute Lung Inflammation Induced by Cigarette Smoke in the Mouse. *Phytomedicine*. **2012**; *19*(3), 262-269.

67) Mertens-Talcott, S. U.; Rios, J.; Jilma-Stohlawetz, P.; Pacheco-Palencia, L. A.; Meibohm, B.; Talcott, S. T.; Derendorf, H. Pharmacokinetics of Anthocyanins and Antioxidant Effects After the Consumption of Anthocyanin-Rich Acai Juice and Pulp (Euterpe oleracea Mart.) in Human Healthy Volunteers. *J. Agric. Food Chem*., **2008**, *56*(17), 7796- 7802.

68) Showande, S. S.; Fakeye, T. O.; Tolonen, A; Hokkanen, J. *In vitro* Inhibitory Activities of the Extract of *Hibiscus sabdariffa* on selected Cytochrome P450 Isoforms. *Afr. J. Trad. Comp. Alt. Med*., **2013**. *10*(3). 533-540.

69) Phillipson, D. W.; Milgram, K. E.; Yanovsky, A. I.; Rusnak, L. S.; Haggerty, D. A.; Farrell, W. P.; Greig, M. J.; Xiong, X.; Proefke, M. L. High-Throughput Bioassayguided Fractionation: A Technique for Rapidly Assigning Observed Activity to Individual Components of Combinatorial Libraries, Screened in HTS Bioassays. *J. Comb. Chem.*, **2002**, 4*(*6), 591-599.

70) Oberlies, N. H.; Kroll, D. J. Camptothecin and Taxol: Historic Achievements in Natural Products *Research. J. Nat. Prod*., **2004**, *67*(2), 129-135.

71) Yamazaki, H.; Masaak, T.; Shimada, T. Highly Sensitive High-Performance Liquid Chromatographic Assay for Coumarin 7-Hydroxylation and 7-Ethoxycoumarin O-Deethylation by Human Liver Cytochrome P450 Enzymes. *J. Chromatogr. B.*, **1999**, *721*(1), 13-19.

72) Cholerton, S.; Idle, M. E.; Vas, A.; Gonzalez, F. J.; Idle, J. R. Comparison of a Novel Thin-Layer Chromatographic-Fluorescence Detection Method with a

Spectrofluorometric Method for the Determination of 7-Hydroxycoumarin in Human Urine. *J. Chromatogr.*, **1992**, *575*(2), 325-330.

73) Ciolino H.; Wang T. T. Y.; Chao Yeh G. Diosmin and Diosmetin are Agonists of the Aryl Hydrocarbon Receptor That Differentially Affect Cytochrome P450 1A1 Activity. *Cancer Res.*, **1998**, *58*, 2754-2760.

74) Iordachescu A.; Silvestro L.; Rizea Savu S.; Tarcomnicu I.; Moise A. Diosmetin Pharmacokinetic Following Diosmin Oral Administration in Man; A New Study on an Old Product with Controversial Pharmacokinetic Findings in the Past. *J. Bioequiv. Availab.*, **2012**, *4*(3), 70.